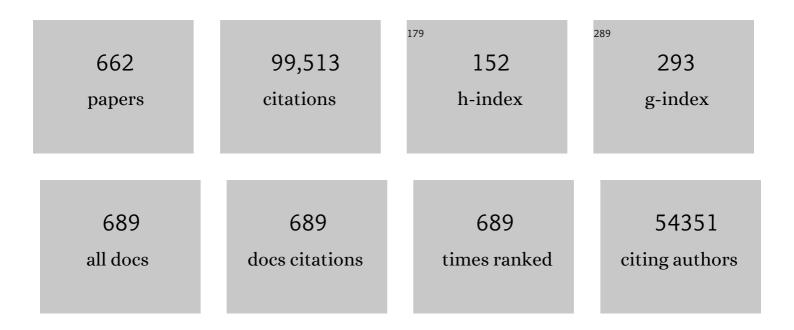
Joseph T Hupp

List of Publications by Year in descending order

Source: https://exaly.com/author-pdf/9088003/publications.pdf

Version: 2024-02-01



LOSEDH T HUDD

#	Article	IF	CITATIONS
1	Metal–organic framework materials as catalysts. Chemical Society Reviews, 2009, 38, 1450.	18.7	7,228
2	Metal–Organic Framework Materials as Chemical Sensors. Chemical Reviews, 2012, 112, 1105-1125.	23.0	6,221
3	Imparting functionality to a metal–organic framework material by controlled nanoparticle encapsulation. Nature Chemistry, 2012, 4, 310-316.	6.6	1,857
4	2D Homologous Perovskites as Light-Absorbing Materials for Solar Cell Applications. Journal of the American Chemical Society, 2015, 137, 7843-7850.	6.6	1,818
5	Ruddlesden–Popper Hybrid Lead Iodide Perovskite 2D Homologous Semiconductors. Chemistry of Materials, 2016, 28, 2852-2867.	3.2	1,607
6	De novo synthesis of a metal–organic framework material featuring ultrahigh surface area and gas storage capacities. Nature Chemistry, 2010, 2, 944-948.	6.6	1,535
7	Metal–Organic Framework Materials with Ultrahigh Surface Areas: Is the Sky the Limit?. Journal of the American Chemical Society, 2012, 134, 15016-15021.	6.6	1,497
8	Chemical, thermal and mechanical stabilities of metal–organic frameworks. Nature Reviews Materials, 2016, 1, .	23.3	1,490
9	A facile synthesis of UiO-66, UiO-67 and their derivatives. Chemical Communications, 2013, 49, 9449.	2.2	1,340
10	Rational Design, Synthesis, Purification, and Activation of Metalâ^'Organic Framework Materials. Accounts of Chemical Research, 2010, 43, 1166-1175.	7.6	1,259
11	Large-scale screening of hypothetical metal–organic frameworks. Nature Chemistry, 2012, 4, 83-89.	6.6	1,098
12	Metalâ^'Organic Frameworks as Sensors: A ZIF-8 Based Fabryâ^'Pérot Device as a Selective Sensor for Chemical Vapors and Gases. Journal of the American Chemical Society, 2010, 132, 7832-7833.	6.6	981
13	A metal–organic framework material that functions as an enantioselective catalyst for olefin epoxidation. Chemical Communications, 2006, , 2563-2565.	2.2	920
14	Gold Nanoparticle-Based Sensing of "Spectroscopically Silent―Heavy Metal Ions. Nano Letters, 2001, 1, 165-167.	4.5	866
15	Methane Storage in Metal–Organic Frameworks: Current Records, Surprise Findings, and Challenges. Journal of the American Chemical Society, 2013, 135, 11887-11894.	6.6	841
16	Vapor-Phase Metalation by Atomic Layer Deposition in a Metal–Organic Framework. Journal of the American Chemical Society, 2013, 135, 10294-10297.	6.6	821
17	Porous Organic Polymers in Catalysis: Opportunities and Challenges. ACS Catalysis, 2011, 1, 819-835.	5.5	818
18	Destruction of chemical warfare agents using metal–organic frameworks. Nature Materials, 2015, 14, 512-516.	13.3	790

#	Article	IF	CITATIONS
19	ZnO Nanotube Based Dye-Sensitized Solar Cells. Nano Letters, 2007, 7, 2183-2187.	4.5	730
20	Beyond post-synthesis modification: evolution of metal–organic frameworks via building block replacement. Chemical Society Reviews, 2014, 43, 5896-5912.	18.7	721
21	Metal–organic frameworks for the removal of toxic industrial chemicals and chemical warfare agents. Chemical Society Reviews, 2017, 46, 3357-3385.	18.7	707
22	Light-Harvesting Metal–Organic Frameworks (MOFs): Efficient Strut-to-Strut Energy Transfer in Bodipy and Porphyrin-Based MOFs. Journal of the American Chemical Society, 2011, 133, 15858-15861.	6.6	702
23	Advancing beyond current generation dye-sensitized solar cells. Energy and Environmental Science, 2008, 1, 66.	15.6	663
24	Postsynthetic Tuning of Metal–Organic Frameworks for Targeted Applications. Accounts of Chemical Research, 2017, 50, 805-813.	7.6	644
25	Fe-Porphyrin-Based Metal–Organic Framework Films as High-Surface Concentration, Heterogeneous Catalysts for Electrochemical Reduction of CO ₂ . ACS Catalysis, 2015, 5, 6302-6309.	5.5	639
26	Chemical Reduction of Metalâ^'Organic Framework Materials as a Method to Enhance Gas Uptake and Binding. Journal of the American Chemical Society, 2007, 129, 9604-9605.	6.6	591
27	Separation of CO ₂ from CH ₄ Using Mixed-Ligand Metalâ^'Organic Frameworks. Langmuir, 2008, 24, 8592-8598.	1.6	557
28	A Catalytically Active, Permanently Microporous MOF with Metalloporphyrin Struts. Journal of the American Chemical Society, 2009, 131, 4204-4205.	6.6	526
29	Synthesis and Optical Properties of "Branched―Gold Nanocrystals. Nano Letters, 2004, 4, 327-330.	4.5	524
30	Best Practices for the Synthesis, Activation, and Characterization of Metal–Organic Frameworks. Chemistry of Materials, 2017, 29, 26-39.	3.2	518
31	Light-Harvesting and Ultrafast Energy Migration in Porphyrin-Based Metal–Organic Frameworks. Journal of the American Chemical Society, 2013, 135, 862-869.	6.6	510
32	Supercritical Processing as a Route to High Internal Surface Areas and Permanent Microporosity in Metalâ^'Organic Framework Materials. Journal of the American Chemical Society, 2009, 131, 458-460.	6.6	474
33	Perfluoroalkane Functionalization of NU-1000 via Solvent-Assisted Ligand Incorporation: Synthesis and CO ₂ Adsorption Studies. Journal of the American Chemical Society, 2013, 135, 16801-16804.	6.6	473
34	A Hafnium-Based Metal–Organic Framework as an Efficient and Multifunctional Catalyst for Facile CO ₂ Fixation and Regioselective and Enantioretentive Epoxide Activation. Journal of the American Chemical Society, 2014, 136, 15861-15864.	6.6	470
35	Microporous Pillared Paddle-Wheel Frameworks Based on Mixed-Ligand Coordination of Zinc Ions. Inorganic Chemistry, 2005, 44, 4912-4914.	1.9	447
36	Distance Dependence of Plasmon-Enhanced Photocurrent in Dye-Sensitized Solar Cells. Journal of the American Chemical Society, 2009, 131, 8407-8409.	6.6	434

Joseph T Hupp

#	Article	IF	CITATIONS
37	Active-Site-Accessible, Porphyrinic Metalâ^'Organic Framework Materials. Journal of the American Chemical Society, 2011, 133, 5652-5655.	6.6	415
38	Luminescent sensor molecules based on coordinated metals: a review of recent developments. Coordination Chemistry Reviews, 2000, 205, 201-228.	9.5	414
39	Metal–organic framework materials for light-harvesting and energy transfer. Chemical Communications, 2015, 51, 3501-3510.	2.2	409
40	High Propene/Propane Selectivity in Isostructural Metal–Organic Frameworks with High Densities of Open Metal Sites. Angewandte Chemie - International Edition, 2012, 51, 1857-1860.	7.2	392
41	Coordination-Chemistry Control of Proton Conductivity in the Iconic Metal–Organic Framework Material HKUST-1. Journal of the American Chemical Society, 2012, 134, 51-54.	6.6	382
42	Artificial Enzymes Formed through Directed Assembly of Molecular Square Encapsulated Epoxidation Catalysts. Angewandte Chemie - International Edition, 2001, 40, 4239-4242.	7.2	379
43	Enhancement of CO2/N2 selectivity in a metal-organic framework by cavity modification. Journal of Materials Chemistry, 2009, 19, 2131.	6.7	370
44	Opening ZIF-8: A Catalytically Active Zeolitic Imidazolate Framework of Sodalite Topology with Unsubstituted Linkers. Journal of the American Chemical Society, 2012, 134, 18790-18796.	6.6	370
45	Simple and Compelling Biomimetic Metal–Organic Framework Catalyst for the Degradation of Nerve Agent Simulants. Angewandte Chemie - International Edition, 2014, 53, 497-501.	7.2	364
46	Metal-adeninate vertices for the construction of an exceptionally porous metal-organic framework. Nature Communications, 2012, 3, 604.	5.8	356
47	Carborane-based metal–organic frameworks as highly selective sorbents for CO2 over methane. Chemical Communications, 2008, , 4135.	2.2	349
48	Room-Temperature Synthesis of UiO-66 and Thermal Modulation of Densities of Defect Sites. Chemistry of Materials, 2017, 29, 1357-1361.	3.2	346
49	Thin Films and Solar Cells Based on Semiconducting Two-Dimensional Ruddlesden–Popper (CH ₃ (CH ₂) ₃ NH ₃) ₂ (CH ₃ NH _{ Perovskites. ACS Energy Letters, 2017, 2, 982-990.}	•3≪asanp>)•	≺suabaas <i>n<!--í</td--></i>
50	Control over Catenation in Metalâ^'Organic Frameworks via Rational Design of the Organic Building Block. Journal of the American Chemical Society, 2010, 132, 950-952.	6.6	344
51	Solventâ€Assisted Linker Exchange: An Alternative to the Deâ€Novo Synthesis of Unattainable Metal–Organic Frameworks. Angewandte Chemie - International Edition, 2014, 53, 4530-4540.	7.2	339
52	Instantaneous Hydrolysis of Nerveâ€Agent Simulants with a Sixâ€Connected Zirconiumâ€Based Metal–Organic Framework. Angewandte Chemie - International Edition, 2015, 54, 6795-6799.	7.2	338
53	Structure–property relationships of porous materials for carbon dioxide separation and capture. Energy and Environmental Science, 2012, 5, 9849.	15.6	334
54	High Efficiency Adsorption and Removal of Selenate and Selenite from Water Using Metal–Organic Frameworks. Journal of the American Chemical Society, 2015, 137, 7488-7494.	6.6	330

#	Article	IF	CITATIONS
55	Ultrahigh Surface Area Zirconium MOFs and Insights into the Applicability of the BET Theory. Journal of the American Chemical Society, 2015, 137, 3585-3591.	6.6	329
56	Energy Transfer from Quantum Dots to Metal–Organic Frameworks for Enhanced Light Harvesting. Journal of the American Chemical Society, 2013, 135, 955-958.	6.6	328
57	Supramolecular Coordination Chemistry and Functional Microporous Molecular Materials. Chemistry of Materials, 2001, 13, 3113-3125.	3.2	320
58	Metalâ^'Organic Framework Thin Film for Enhanced Localized Surface Plasmon Resonance Gas Sensing. Analytical Chemistry, 2010, 82, 8042-8046.	3.2	317
59	Luminescent transition-metal-containing cyclophanes ("molecular squaresâ€): covalent self-assembly, host-guest studies and preliminary nanoporous materials applications. Coordination Chemistry Reviews, 1998, 171, 221-243.	9.5	313
60	Post-Synthesis Alkoxide Formation Within Metalâ^'Organic Framework Materials: A Strategy for Incorporating Highly Coordinatively Unsaturated Metal Ions. Journal of the American Chemical Society, 2009, 131, 3866-3868.	6.6	302
61	Encapsulation of a Nerve Agent Detoxifying Enzyme by a Mesoporous Zirconium Metal–Organic Framework Engenders Thermal and Long-Term Stability. Journal of the American Chemical Society, 2016, 138, 8052-8055.	6.6	302
62	Urea Metal–Organic Frameworks as Effective and Size-Selective Hydrogen-Bond Catalysts. Journal of the American Chemical Society, 2012, 134, 3334-3337.	6.6	292
63	Catalytic Zirconium/Hafnium-Based Metal–Organic Frameworks. ACS Catalysis, 2017, 7, 997-1014.	5.5	288
64	Optical Properties of Metal Nanoshells. Journal of Physical Chemistry B, 2004, 108, 1224-1229.	1.2	282
65	Methane Oxidation to Methanol Catalyzed by Cu-Oxo Clusters Stabilized in NU-1000 Metal–Organic Framework. Journal of the American Chemical Society, 2017, 139, 10294-10301.	6.6	282
66	Are Zr ₆ -based MOFs water stable? Linker hydrolysis vs. capillary-force-driven channel collapse. Chemical Communications, 2014, 50, 8944.	2.2	277
67	Scalable synthesis and post-modification of a mesoporous metal-organic framework called NU-1000. Nature Protocols, 2016, 11, 149-162.	5.5	276
68	Catalytic degradation of chemical warfare agents and their simulants by metal-organic frameworks. Coordination Chemistry Reviews, 2017, 346, 101-111.	9.5	275
69	Synthesis and Optical Properties of Anisotropic Metal Nanoparticles. Journal of Fluorescence, 2004, 14, 331-341.	1.3	273
70	Sintering-Resistant Single-Site Nickel Catalyst Supported by Metal–Organic Framework. Journal of the American Chemical Society, 2016, 138, 1977-1982.	6.6	273
71	Synthesis, Properties, and Gas Separation Studies of a Robust Diimide-Based Microporous Organic Polymer. Chemistry of Materials, 2009, 21, 3033-3035.	3.2	272
72	Synthesis and Hydrogen Sorption Properties of Carborane Based Metalâ^'Organic Framework Materials. Journal of the American Chemical Society, 2007, 129, 12680-12681.	6.6	269

#	Article	IF	CITATIONS
73	Temperature Treatment of Highly Porous Zirconium-Containing Metal–Organic Frameworks Extends Drug Delivery Release. Journal of the American Chemical Society, 2017, 139, 7522-7532.	6.6	269
74	Transmetalation: routes to metal exchange within metal–organic frameworks. Journal of Materials Chemistry A, 2013, 1, 5453.	5.2	267
75	Directed Growth of Electroactive Metalâ€Organic Framework Thin Films Using Electrophoretic Deposition. Advanced Materials, 2014, 26, 6295-6300.	11.1	265
76	Exploiting parameter space in MOFs: a 20-fold enhancement of phosphate-ester hydrolysis with UiO-66-NH ₂ . Chemical Science, 2015, 6, 2286-2291.	3.7	265
77	Remnant PbI2, an unforeseen necessity in high-efficiency hybrid perovskite-based solar cells?. APL Materials, 2014, 2, .	2.2	264
78	Kinetic Separation of Propene and Propane in Metalâ~'Organic Frameworks: Controlling Diffusion Rates in Plate-Shaped Crystals via Tuning of Pore Apertures and Crystallite Aspect Ratios. Journal of the American Chemical Society, 2011, 133, 5228-5231.	6.6	263
79	Luminescent Rhenium/Palladium Square Complex Exhibiting Excited State Intramolecular Electron Transfer Reactivity and Molecular Anion Sensing Characteristics. Journal of the American Chemical Society, 1995, 117, 11813-11814.	6.6	261
80	Evaluation of BrÃ,nsted acidity and proton topology in Zr- and Hf-based metal–organic frameworks using potentiometric acid–base titration. Journal of Materials Chemistry A, 2016, 4, 1479-1485.	5.2	259
81	Mechanochemical and solvent-free assembly of zirconium-based metal–organic frameworks. Chemical Communications, 2016, 52, 2133-2136.	2.2	256
82	Electron Transport in Dye-Sensitized Solar Cells Based on ZnO Nanotubes: Evidence for Highly Efficient Charge Collection and Exceptionally Rapid Dynamics. Journal of Physical Chemistry A, 2009, 113, 4015-4021.	1.1	255
83	Incorporation of an A1/A2-Difunctionalized Pillar[5]arene into a Metal–Organic Framework. Journal of the American Chemical Society, 2012, 134, 17436-17439.	6.6	254
84	New Architectures for Dye‧ensitized Solar Cells. Chemistry - A European Journal, 2008, 14, 4458-4467.	1.7	253
85	Melt-Quenched Glasses of Metal–Organic Frameworks. Journal of the American Chemical Society, 2016, 138, 3484-3492.	6.6	252
86	Layer-by-Layer Fabrication of Oriented Porous Thin Films Based on Porphyrin-Containing Metal–Organic Frameworks. Journal of the American Chemical Society, 2013, 135, 15698-15701.	6.6	250
87	Prospects for nanoporous metal-organic materials in advanced separations processes. AICHE Journal, 2004, 50, 1090-1095.	1.8	249
88	Selective Photooxidation of a Mustardâ€Gas Simulant Catalyzed by a Porphyrinic Metal–Organic Framework. Angewandte Chemie - International Edition, 2015, 54, 9001-9005.	7.2	244
89	Post-Synthesis Modification of a Metal–Organic Framework To Form Metallosalen-Containing MOF Materials. Journal of the American Chemical Society, 2011, 133, 13252-13255.	6.6	243
90	Metal–Organic Framework Thin Films Composed of Free-Standing Acicular Nanorods Exhibiting Reversible Electrochromism. Chemistry of Materials, 2013, 25, 5012-5017.	3.2	242

#	Article	IF	CITATIONS
91	Activation of metal–organic framework materials. CrystEngComm, 2013, 15, 9258.	1.3	239
92	A porous proton-relaying metal-organic framework material that accelerates electrochemical hydrogen evolution. Nature Communications, 2015, 6, 8304.	5.8	239
93	Enzyme encapsulation in metal–organic frameworks for applications in catalysis. CrystEngComm, 2017, 19, 4082-4091.	1.3	235
94	Synthesis, Characterization, and Preliminary Hostâ´'Guest Binding Studies of Porphyrinic Molecular Squares Featuringfac-Tricarbonylrhenium(I) Chloro Corners. Inorganic Chemistry, 1997, 36, 5422-5423.	1.9	232
95	Evaluating topologically diverse metal–organic frameworks for cryo-adsorbed hydrogen storage. Energy and Environmental Science, 2016, 9, 3279-3289.	15.6	231
96	In silico discovery of metal-organic frameworks for precombustion CO ₂ capture using a genetic algorithm. Science Advances, 2016, 2, e1600909.	4.7	231
97	Toward Plasmonic Solar Cells: Protection of Silver Nanoparticles via Atomic Layer Deposition of TiO ₂ . Langmuir, 2009, 25, 2596-2600.	1.6	230
98	Defining the Proton Topology of the Zr ₆ -Based Metal–Organic Framework NU-1000. Journal of Physical Chemistry Letters, 2014, 5, 3716-3723.	2.1	228
99	Metal–Organic Framework Nodes as Nearly Ideal Supports for Molecular Catalysts: NU-1000- and UiO-66-Supported Iridium Complexes. Journal of the American Chemical Society, 2015, 137, 7391-7396.	6.6	228
100	Metalââ,¬â€œOrganic Framework-Based Catalysts: Chemical Fixation of CO2 with Epoxides Leading to Cyclic Organic Carbonates. Frontiers in Energy Research, 2015, 2, .	1.2	225
101	Selective Bifunctional Modification of a Non-catenated Metalâ^'Organic Framework Material via "Click―Chemistry. Journal of the American Chemical Society, 2009, 131, 13613-13615.	6.6	224
102	Metal–Organic Framework Supported Cobalt Catalysts for the Oxidative Dehydrogenation of Propane at Low Temperature. ACS Central Science, 2017, 3, 31-38.	5.3	222
103	Gram-scale, high-yield synthesis of a robust metal–organic framework for storing methane and other gases. Energy and Environmental Science, 2013, 6, 1158.	15.6	219
104	Quadratic Nonlinear Optical Properties ofN-Aryl Stilbazolium Dyes. Advanced Functional Materials, 2002, 12, 110-116.	7.8	218
105	A Metal–Organic Framework-Based Material for Electrochemical Sensing of Carbon Dioxide. Journal of the American Chemical Society, 2014, 136, 8277-8282.	6.6	218
106	Self-Assembly of Luminescent Molecular Squares Featuring Octahedral Rhenium Corners. Inorganic Chemistry, 1996, 35, 4096-4097.	1.9	216
107	Surface Modification of SnO ₂ Photoelectrodes in Dye-Sensitized Solar Cells: Significant Improvements in Photovoltage via Al ₂ O ₃ Atomic Layer Deposition. Journal of Physical Chemistry Letters, 2010, 1, 1611-1615.	2.1	216
108	Synthesis of Silver Nanodisks Using Polystyrene Mesospheres as Templates. Journal of the American Chemical Society, 2002, 124, 15182-15183.	6.6	215

#	Article	IF	CITATIONS
109	Engineering ZIFâ€8 Thin Films for Hybrid MOFâ€Based Devices. Advanced Materials, 2012, 24, 3970-3974.	11.1	213
110	Dye Sensitized Solar Cells: TiO ₂ Sensitization with a Bodipy-Porphyrin Antenna System. Langmuir, 2010, 26, 3760-3765.	1.6	211
111	An Exceptionally Stable Metal–Organic Framework Supported Molybdenum(VI) Oxide Catalyst for Cyclohexene Epoxidation. Journal of the American Chemical Society, 2016, 138, 14720-14726.	6.6	211
112	Energetics of the Nanocrystalline Titanium Dioxide/Aqueous Solution Interface:  Approximate Conduction Band Edge Variations between H0 = â^'10 and H- = +26. Journal of Physical Chemistry B, 1999, 103, 4623-4628.	1.2	210
113	Framework-Topology-Dependent Catalytic Activity of Zirconium-Based (Porphinato)zinc(II) MOFs. Journal of the American Chemical Society, 2016, 138, 14449-14457.	6.6	210
114	Toward solar fuels: Water splitting with sunlight and "rust�. Coordination Chemistry Reviews, 2012, 256, 2521-2529.	9.5	209
115	Versatile functionalization of the NU-1000 platform by solvent-assisted ligand incorporation. Chemical Communications, 2014, 50, 1965.	2.2	208
116	Dual-Function Metal–Organic Framework as a Versatile Catalyst for Detoxifying Chemical Warfare Agent Simulants. ACS Nano, 2015, 9, 12358-12364.	7.3	207
117	Vanadium-Node-Functionalized UiO-66: A Thermally Stable MOF-Supported Catalyst for the Gas-Phase Oxidative Dehydrogenation of Cyclohexene. ACS Catalysis, 2014, 4, 2496-2500.	5.5	206
118	Rhenium-Based Molecular Rectangles as Frameworks for Ligand-Centered Mixed Valency and Optical Electron Transfer. Journal of the American Chemical Society, 2004, 126, 12989-13001.	6.6	204
119	Nanosizing a Metal–Organic Framework Enzyme Carrier for Accelerating Nerve Agent Hydrolysis. ACS Nano, 2016, 10, 9174-9182.	7.3	202
120	Semiconductor-Based Interfacial Electron-Transfer Reactivity:Â Decoupling Kinetics from pH-Dependent Band Energetics in a Dye-Sensitized Titanium Dioxide/Aqueous Solution System. The Journal of Physical Chemistry, 1996, 100, 6867-6870.	2.9	201
121	Application of Consistency Criteria To Calculate BET Areas of Micro- And Mesoporous Metal–Organic Frameworks. Journal of the American Chemical Society, 2016, 138, 215-224.	6.6	201
122	Designing Higher Surface Area Metal–Organic Frameworks: Are Triple Bonds Better Than Phenyls?. Journal of the American Chemical Society, 2012, 134, 9860-9863.	6.6	198
123	Synthesis of nanocrystals of Zr-based metal–organic frameworks with csq-net: significant enhancement in the degradation of a nerve agent simulant. Chemical Communications, 2015, 51, 10925-10928.	2.2	194
124	Dynamics of charge transport and recombination in ZnO nanorod array dye-sensitized solar cells. Physical Chemistry Chemical Physics, 2006, 8, 4655.	1.3	193
125	An Interpenetrated Framework Material with Hysteretic CO ₂ Uptake. Chemistry - A European Journal, 2010, 16, 276-281.	1.7	192
126	Computational Design of Metal–Organic Frameworks Based on Stable Zirconium Building Units for Storage and Delivery of Methane. Chemistry of Materials, 2014, 26, 5632-5639.	3.2	191

#	Article	IF	CITATIONS
127	Directed Assembly of Transition-Metal-Coordinated Molecular Loops and Squares from Salen-Type Components. Examples of Metalation-Controlled Structural Conversion. Journal of the American Chemical Society, 2004, 126, 6314-6326.	6.6	190
128	Ni(III)/(IV) Bis(dicarbollide) as a Fast, Noncorrosive Redox Shuttle for Dye-Sensitized Solar Cells. Journal of the American Chemical Society, 2010, 132, 4580-4582.	6.6	190
129	Turning On Catalysis: Incorporation of a Hydrogen-Bond-Donating Squaramide Moiety into a Zr Metal–Organic Framework. Journal of the American Chemical Society, 2015, 137, 919-925.	6.6	186
130	The dual capture of As ^V and As ^{III} by UiO-66 and analogues. Chemical Science, 2016, 7, 6492-6498.	3.7	181
131	Single-Atom-Based Vanadium Oxide Catalysts Supported on Metal–Organic Frameworks: Selective Alcohol Oxidation and Structure–Activity Relationship. Journal of the American Chemical Society, 2018, 140, 8652-8656.	6.6	181
132	MOF Functionalization via Solvent-Assisted Ligand Incorporation: Phosphonates vs Carboxylates. Inorganic Chemistry, 2015, 54, 2185-2192.	1.9	177
133	Probing the correlations between the defects in metal–organic frameworks and their catalytic activity by an epoxide ring-opening reaction. Chemical Communications, 2016, 52, 7806-7809.	2.2	177
134	Molecular Rectangles Based on Rhenium(I) Coordination Chemistry. Journal of the American Chemical Society, 1998, 120, 12982-12983.	6.6	176
135	Alkali Metal Cation Effects on Hydrogen Uptake and Binding in Metal-Organic Frameworks. Inorganic Chemistry, 2008, 47, 7936-7938.	1.9	175
136	Design and Synthesis of a Water‣table Anionic Uraniumâ€Based Metal–Organic Framework (MOF) with Ultra Large Pores. Angewandte Chemie - International Edition, 2016, 55, 10358-10362.	7.2	175
137	Zirconium-Based Metal–Organic Frameworks for the Catalytic Hydrolysis of Organophosphorus Nerve Agents. ACS Applied Materials & Interfaces, 2020, 12, 14702-14720.	4.0	175
138	Mucin-Pseudomonas aeruginosa interactions promote biofilm formation and antibiotic resistance. Molecular Microbiology, 2006, 59, 142-151.	1.2	173
139	Porphyrin-containing molecular squares: Design and applications. Coordination Chemistry Reviews, 2006, 250, 1710-1723.	9.5	171
140	Porphyrin-based metal–organic framework thin films for electrochemical nitrite detection. Electrochemistry Communications, 2015, 58, 51-56.	2.3	171
141	Fabrication of Metalâ€Organic Frameworkâ€Containing Silicaâ€Colloidal Crystals for Vapor Sensing. Advanced Materials, 2011, 23, 4449-4452.	11.1	170
142	Outer-Sphere Redox Couples as Shuttles in Dye-Sensitized Solar Cells. Performance Enhancement Based on Photoelectrode Modification via Atomic Layer Deposition. Journal of Physical Chemistry C, 2008, 112, 19756-19764.	1.5	168
143	Synthesis of catalytically active porous organic polymers from metalloporphyrin building blocks. Chemical Science, 2011, 2, 686.	3.7	168
144	Metal–organic framework (MOF) materials as polymerization catalysts: a review and recent advances. Chemical Communications, 2020, 56, 10409-10418.	2.2	168

#	Article	IF	CITATIONS
145	Synthesis and characterization of isostructural cadmium zeolitic imidazolate frameworks via solvent-assisted linker exchange. Chemical Science, 2012, 3, 3256.	3.7	166
146	Photocurrent Enhancement by Surface Plasmon Resonance of Silver Nanoparticles in Highly Porous Dye-Sensitized Solar Cells. Langmuir, 2011, 27, 14609-14614.	1.6	165
147	Cavity-Tailored, Self-Sorting Supramolecular Catalytic Boxes for Selective Oxidation. Journal of the American Chemical Society, 2008, 130, 16828-16829.	6.6	164
148	CHEMISTRY: Enhanced: Better Living Through Nanopore Chemistry. Science, 2005, 309, 2008-2009.	6.0	161
149	Atomically Precise Growth of Catalytically Active Cobalt Sulfide on Flat Surfaces and within a Metal–Organic Framework <i>via</i> Atomic Layer Deposition. ACS Nano, 2015, 9, 8484-8490.	7.3	158
150	Increased Electrical Conductivity in a Mesoporous Metal–Organic Framework Featuring Metallacarboranes Guests. Journal of the American Chemical Society, 2018, 140, 3871-3875.	6.6	158
151	A porous, electrically conductive hexa-zirconium(<scp>iv</scp>) metal–organic framework. Chemical Science, 2018, 9, 4477-4482.	3.7	158
152	Tailoring the Pore Size and Functionality of UiO-Type Metal–Organic Frameworks for Optimal Nerve Agent Destruction. Inorganic Chemistry, 2015, 54, 9684-9686.	1.9	157
153	Copper Nanoparticles Installed in Metal–Organic Framework Thin Films are Electrocatalytically Competent for CO ₂ Reduction. ACS Energy Letters, 2017, 2, 2394-2401.	8.8	157
154	A "click-based―porous organic polymer from tetrahedral building blocks. Journal of Materials Chemistry, 2011, 21, 1700.	6.7	156
155	Selective isolation of gold facilitated by second-sphere coordination with α-cyclodextrin. Nature Communications, 2013, 4, 1855.	5.8	156
156	Covalent surface modification of a metal–organic framework: selective surface engineering via Cul-catalyzed Huisgen cycloaddition. Chemical Communications, 2008, , 5493.	2.2	155
157	Tuning the Surface Chemistry of Metal Organic Framework Nodes: Proton Topology of the Metal-Oxide-Like Zr ₆ Nodes of UiO-66 and NU-1000. Journal of the American Chemical Society, 2016, 138, 15189-15196.	6.6	155
158	Atomic layer deposition of tin oxide films using tetrakis(dimethylamino) tin. Journal of Vacuum Science and Technology A: Vacuum, Surfaces and Films, 2008, 26, 244-252.	0.9	153
159	Enormous Hyper-Rayleigh Scattering from Nanocrystalline Gold Particle Suspensions. Journal of Physical Chemistry B, 1998, 102, 10091-10093.	1.2	151
160	Toward Inexpensive Photocatalytic Hydrogen Evolution: A Nickel Sulfide Catalyst Supported on a High-Stability Metal–Organic Framework. ACS Applied Materials & Interfaces, 2016, 8, 20675-20681.	4.0	151
161	Electronic Coherence, Vibrational Coherence, and Solvent Degrees of Freedom in the Femtosecond Spectroscopy of Mixed-Valence Metal Dimers in H2O and D2O. The Journal of Physical Chemistry, 1995, 99, 2609-2616.	2.9	150
162	Waterâ€Stable Zirconiumâ€Based Metal–Organic Framework Material with Highâ€Surface Area and Gasâ€Storage Capacities. Chemistry - A European Journal, 2014, 20, 12389-12393.	1.7	150

#	Article	IF	CITATIONS
163	Tuning Zr ₆ Metal–Organic Framework (MOF) Nodes as Catalyst Supports: Site Densities and Electron-Donor Properties Influence Molecular Iridium Complexes as Ethylene Conversion Catalysts. ACS Catalysis, 2016, 6, 235-247.	5.5	150
164	A Zn-based, pillared paddlewheel MOF containing free carboxylic acids via covalent post-synthesis elaboration. Chemical Communications, 2009, , 3720.	2.2	149
165	Ultraporous, Water Stable, and Breathing Zirconium-Based Metal–Organic Frameworks with ftw Topology. Journal of the American Chemical Society, 2015, 137, 13183-13190.	6.6	149
166	MOF-enabled confinement and related effects for chemical catalyst presentation and utilization. Chemical Society Reviews, 2022, 51, 1045-1097.	18.7	148
167	Enhanced Catalytic Activity through the Tuning of Micropore Environment and Supercritical CO ₂ Processing: Al(Porphyrin)-Based Porous Organic Polymers for the Degradation of a Nerve Agent Simulant. Journal of the American Chemical Society, 2013, 135, 11720-11723.	6.6	147
168	Efficient and selective oxidation of sulfur mustard using singlet oxygen generated by a pyrene-based metal–organic framework. Journal of Materials Chemistry A, 2016, 4, 13809-13813.	5.2	147
169	Benchmark Study of Hydrogen Storage in Metal–Organic Frameworks under Temperature and Pressure Swing Conditions. ACS Energy Letters, 2018, 3, 748-754.	8.8	147
170	Surfaceâ€Specific Functionalization of Nanoscale Metal–Organic Frameworks. Angewandte Chemie - International Edition, 2015, 54, 14738-14742.	7.2	146
171	Thin-Film Molecular Materials Based on Tetrametallic "Squaresâ€ŧ Nanoscale Porosity and Size-Selective Guest Transport Characteristics. Journal of the American Chemical Society, 1999, 121, 557-563.	6.6	145
172	Singlet and Triplet Excited States of Emissive, Conjugated Bis(porphyrin) Compounds Probed by Optical and EPR Spectroscopic Methods. Journal of the American Chemical Society, 2000, 122, 7017-7033.	6.6	145
173	Metal–Organic Framework Thin Films as Platforms for Atomic Layer Deposition of Cobalt Ions To Enable Electrocatalytic Water Oxidation. ACS Applied Materials & Interfaces, 2015, 7, 28223-28230.	4.0	145
174	Chemical reduction of a diimide based porous polymer for selective uptake of carbon dioxide versus methane. Chemical Communications, 2010, 46, 1056.	2.2	144
175	Adsorption of a Catalytically Accessible Polyoxometalate in a Mesoporous Channel-type Metal–Organic Framework. Chemistry of Materials, 2017, 29, 5174-5181.	3.2	143
176	Hyper-Rayleigh scattering studies of silver, copper, and platinum nanoparticle suspensions. Chemical Physics Letters, 2002, 356, 534-540.	1.2	142
177	Solvent-assisted linker exchange (SALE) and post-assembly metallation in porphyrinic metal–organic framework materials. Chemical Science, 2013, 4, 1509.	3.7	142
178	Nonlinear Optical Properties of Molecularly Bridged Gold Nanoparticle Arrays. Journal of the American Chemical Society, 2000, 122, 12029-12030.	6.6	141
179	Surface Passivation of Nanoporous TiO ₂ via Atomic Layer Deposition of ZrO ₂ for Solid-State Dye-Sensitized Solar Cell Applications. Journal of Physical Chemistry C, 2009, 113, 18385-18390.	1.5	141
180	Microporous Supramolecular Coordination Compounds as Chemosensory Photonic Lattices. Angewandte Chemie - International Edition, 2002, 41, 154-157.	7.2	139

#	Article	IF	CITATIONS
181	Real-Time Multicolor DNA Detection with Chemoresponsive Diffraction Gratings and Nanoparticle Probes. Journal of the American Chemical Society, 2003, 125, 13541-13547.	6.6	138
182	Aerogel Templated ZnO Dye‧ensitized Solar Cells. Advanced Materials, 2008, 20, 1560-1564.	11.1	138
183	Simultaneously high gravimetric and volumetric methane uptake characteristics of the metal–organic framework NU-111. Chemical Communications, 2013, 49, 2992.	2.2	137
184	A Hafnium-Based Metal–Organic Framework as a Nature-Inspired Tandem Reaction Catalyst. Journal of the American Chemical Society, 2015, 137, 13624-13631.	6.6	137
185	Separation of gas mixtures using Co(ii) carborane-based porous coordination polymers. Chemical Communications, 2010, 46, 3478.	2.2	135
186	Control over Catenation in Pillared Paddlewheel Metal–Organic Framework Materials via Solvent-Assisted Linker Exchange. Chemistry of Materials, 2013, 25, 739-744.	3.2	135
187	Cerium(IV) vs Zirconium(IV) Based Metal–Organic Frameworks for Detoxification of a Nerve Agent. Chemistry of Materials, 2017, 29, 2672-2675.	3.2	135
188	A UiO-66 analogue with uncoordinated carboxylic acids for the broad-spectrum removal of toxic chemicals. New Journal of Chemistry, 2015, 39, 2396-2399.	1.4	133
189	Metal–organic frameworks for applications in remediation of oxyanion/cation-contaminated water. CrystEngComm, 2015, 17, 7245-7253.	1.3	133
190	Solvent, ligand, and ionic charge effects on reaction entropies for simple transition-metal redox couples. Inorganic Chemistry, 1984, 23, 3639-3644.	1.9	132
191	Gasâ€Sorption Properties of Cobalt(II)–Carboraneâ€Based Coordination Polymers as a Function of Morphology. Small, 2009, 5, 1727-1731.	5.2	132
192	Effective, Facile, and Selective Hydrolysis of the Chemical Warfare Agent VX Using Zr ₆ -Based Metal–Organic Frameworks. Inorganic Chemistry, 2015, 54, 10829-10833.	1.9	132
193	Electronic Stark Effect Studies of a Porphyrin-Based Pushâ^'Pull Chromophore Displaying a Large First Hyperpolarizability:  State-Specific Contributions to β. Journal of the American Chemical Society, 1998, 120, 2606-2611.	6.6	131
194	Selective Methane Oxidation to Methanol on Cu-Oxo Dimers Stabilized by Zirconia Nodes of an NU-1000 Metal–Organic Framework. Journal of the American Chemical Society, 2019, 141, 9292-9304.	6.6	131
195	Radial Electron Collection in Dye-Sensitized Solar Cells. Nano Letters, 2008, 8, 2862-2866.	4.5	130
196	Metal–Organic Frameworks as Platform Materials for Solar Fuels Catalysis. ACS Energy Letters, 2018, 3, 598-611.	8.8	130
197	Hyper-Rayleigh scattering from silver nanoparticles. Journal of Chemical Physics, 2002, 117, 5963-5966.	1.2	128
198	Enhancement of CO2/CH4 selectivity in metal-organic frameworks containing lithium cations. Microporous and Mesoporous Materials, 2011, 141, 231-235.	2.2	128

#	Article	IF	CITATIONS
199	The frequency factor for outer-sphere electrochemical reactions. Journal of Electroanalytical Chemistry and Interfacial Electrochemistry, 1983, 152, 1-14.	0.3	127
200	Gas-Phase Dimerization of Ethylene under Mild Conditions Catalyzed by MOF Materials Containing (bpy)Ni ^{II} Complexes. ACS Catalysis, 2015, 5, 6713-6718.	5.5	127
201	Electrochemical Preparation of Molybdenum Trioxide Thin Films:Â Effect of Sintering on Electrochromic and Electroinsertion Properties. Langmuir, 2003, 19, 4316-4326.	1.6	123
202	Interconversion between Free Charges and Bound Excitons in 2D Hybrid Lead Halide Perovskites. Journal of Physical Chemistry C, 2017, 121, 26566-26574.	1.5	123
203	Identification Schemes for Metal–Organic Frameworks To Enable Rapid Search and Cheminformatics Analysis. Crystal Growth and Design, 2019, 19, 6682-6697.	1.4	123
204	Evaluation of the energetics of electron trap states at the nanocrystalline titanium dioxide/aqueous solution interface via time-resolved photoacoustic spectroscopy. Chemical Physics Letters, 2000, 330, 231-236.	1.2	122
205	Atomic Layer Deposition of TiO ₂ on Aerogel Templates: New Photoanodes for Dye-Sensitized Solar Cells. Journal of Physical Chemistry C, 2008, 112, 10303-10307.	1.5	122
206	Electronic Tuning of Nickelâ€Based Bis(dicarbollide) Redox Shuttles in Dyeâ€Sensitized Solar Cells. Angewandte Chemie - International Edition, 2010, 49, 5339-5343.	7.2	121
207	Bias-Switchable Permselectivity and Redox Catalytic Activity of a Ferrocene-Functionalized, Thin-Film Metal–Organic Framework Compound. Journal of Physical Chemistry Letters, 2015, 6, 586-591.	2.1	120
208	Atomic Layer Deposition of In2O3 Using Cyclopentadienyl Indium:  A New Synthetic Route to Transparent Conducting Oxide Films. Chemistry of Materials, 2006, 18, 3571-3578.	3.2	119
209	Intramolecular Energy Transfer within Butadiyne-Linked Chlorophyll and Porphyrin Dimer-Faced, Self-Assembled Prisms. Journal of the American Chemical Society, 2008, 130, 4277-4284.	6.6	119
210	Fast interfacial electron transfer: evidence for inverted region kinetic behavior. Journal of the American Chemical Society, 1993, 115, 4927-4928.	6.6	118
211	An Example of Node-Based Postassembly Elaboration of a Hydrogen-Sorbing, Metalâ~'Organic Framework Material. Inorganic Chemistry, 2008, 47, 10223-10225.	1.9	118
212	Atomic Layer Deposition of Fe ₂ O ₃ Using Ferrocene and Ozone. Journal of Physical Chemistry C, 2011, 115, 4333-4339.	1.5	118
213	Defect Creation by Linker Fragmentation in Metal–Organic Frameworks and Its Effects on Gas Uptake Properties. Inorganic Chemistry, 2014, 53, 6914-6919.	1.9	118
214	Ultrafast measurements on direct photoinduced electron transfer in a mixed-valence complex. The Journal of Physical Chemistry, 1991, 95, 5712-5715.	2.9	117
215	Targeted Single-Site MOF Node Modification: Trivalent Metal Loading via Atomic Layer Deposition. Chemistry of Materials, 2015, 27, 4772-4778.	3.2	116
216	Synthesis and Characterization of Molecular Rectangles Based upon Rhenium Thiolate Dimers. Inorganic Chemistry, 1998, 37, 5404-5405.	1.9	115

#	Article	IF	CITATIONS
217	Carborane-Based Metal–Organic Framework with High Methane and Hydrogen Storage Capacities. Chemistry of Materials, 2013, 25, 3539-3543.	3.2	115
218	Energetics of Semiconductor Electrode/Solution Interfaces: EQCM Evidence for Charge-Compensating Cation Adsorption and Intercalation during Accumulation Layer Formation in the Titanium Dioxide/Acetonitrile System. The Journal of Physical Chemistry, 1995, 99, 15718-15720.	2.9	114
219	A Redox-Active Bistable Molecular Switch Mounted inside a Metal–Organic Framework. Journal of the American Chemical Society, 2016, 138, 14242-14245.	6.6	114
220	Fine-Tuning the Activity of Metal–Organic Framework-Supported Cobalt Catalysts for the Oxidative Dehydrogenation of Propane. Journal of the American Chemical Society, 2017, 139, 15251-15258.	6.6	112
221	Detoxification of a Sulfur Mustard Simulant Using a BODIPY-Functionalized Zirconium-Based Metal–Organic Framework. ACS Applied Materials & Interfaces, 2017, 9, 24555-24560.	4.0	112
222	Growth of Narrowly Dispersed Porphyrin Nanowires and Their Hierarchical Assembly into Macroscopic Columns. Journal of the American Chemical Society, 2008, 130, 9632-9633.	6.6	111
223	Selective Surface and Near-Surface Modification of a Noncatenated, Catalytically Active Metal-Organic Framework Material Based on Mn(salen) Struts. Inorganic Chemistry, 2011, 50, 3174-3176.	1.9	111
224	Framework Reduction and Alkali-Metal Doping of a Triply Catenating Metalâ^`Organic Framework Enhances and Then Diminishes H ₂ Uptake. Langmuir, 2009, 25, 503-508.	1.6	110
225	Opening Metal–Organic Frameworks Vol. 2: Inserting Longer Pillars into Pillared-Paddlewheel Structures through Solvent-Assisted Linker Exchange. Chemistry of Materials, 2013, 25, 3499-3503.	3.2	109
226	Probing the Symmetry of the Nonlinear Optic Chromophore Ru(trans-4,4â€~-diethylaminostyryl-2,2â€~-bipyridine)32+: Insight from Polarized Hyper-Rayleigh Scattering and Electroabsorption (Stark) Spectroscopy. Journal of the American Chemical Society, 1999, 121, 4047-4053.	6.6	108
227	Dye-Sensitized Solar Cells: Driving-Force Effects on Electron Recombination Dynamics with Cobalt-Based Shuttles. Langmuir, 2010, 26, 9082-9087.	1.6	108
228	Cubic and rhombohedral heterobimetallic networks constructed from uranium, transition metals, and phosphonoacetate: new methods for constructing porous materials. Chemical Communications, 2010, 46, 9167.	2.2	108
229	Exploring the Limits of Methane Storage and Delivery in Nanoporous Materials. Journal of Physical Chemistry C, 2014, 118, 6941-6951.	1.5	108
230	Structural Transitions of the Metal-Oxide Nodes within Metal–Organic Frameworks: On the Local Structures of NU-1000 and UiO-66. Journal of the American Chemical Society, 2016, 138, 4178-4185.	6.6	108
231	Using Resonance Raman Spectroscopy To Examine Vibrational Barriers to Electron Transfer and Electronic Delocalization. Accounts of Chemical Research, 2001, 34, 808-817.	7.6	106
232	N-Heterocyclic Carbene-Like Catalysis by a Metal–Organic Framework Material. ACS Catalysis, 2012, 2, 1550-1554.	5.5	106
233	Specific adsorption of halide and pseudohalide ions at electrochemically roughened versus smooth silver-aqueous interfaces. Surface Science, 1983, 125, 429-451.	0.8	104
234	Photophysical and Energy-Transfer Properties of (Salen)zinc Complexes and Supramolecular Assemblies. European Journal of Inorganic Chemistry, 2003, 2003, 2348-2351.	1.0	104

#	Article	IF	CITATIONS
235	Understanding Volumetric and Gravimetric Hydrogen Adsorption Trade-off in Metal–Organic Frameworks. ACS Applied Materials & Interfaces, 2017, 9, 33419-33428.	4.0	104
236	Solâ^'Gel-Encapsulated Alcohol Dehydrogenase as a Versatile, Environmentally Stabilized Sensor for Alcohols and Aldehydes. Journal of the American Chemical Society, 1998, 120, 4366-4371.	6.6	103
237	Class-Encapsulated Light Harvesters: More Efficient Dye-Sensitized Solar Cells by Deposition of Self-Aligned, Conformal, and Self-Limited Silica Layers. Journal of the American Chemical Society, 2012, 134, 9537-9540.	6.6	103
238	SERS of molecules that do not adsorb on Ag surfaces: a metal–organic framework-based functionalization strategy. Analyst, The, 2014, 139, 4073.	1.7	103
239	Single-Site Organozirconium Catalyst Embedded in a Metal–Organic Framework. Journal of the American Chemical Society, 2015, 137, 15680-15683.	6.6	103
240	Node-Accessible Zirconium MOFs. Journal of the American Chemical Society, 2020, 142, 21110-21121.	6.6	103
241	Water stabilization of Zr ₆ -based metal–organic frameworks via solvent-assisted ligand incorporation. Chemical Science, 2015, 6, 5172-5176.	3.7	102
242	High volumetric uptake of ammonia using Cu-MOF-74/Cu-CPO-27. Dalton Transactions, 2016, 45, 4150-4153.	1.6	102
243	Atomic Layer Deposition of Indium Tin Oxide Thin Films Using Nonhalogenated Precursors. Journal of Physical Chemistry C, 2008, 112, 1938-1945.	1.5	101
244	High xenon/krypton selectivity in a metal-organic framework with small pores and strong adsorption sites. Microporous and Mesoporous Materials, 2013, 169, 176-179.	2.2	101
245	Charge Transport in Zirconium-Based Metal–Organic Frameworks. Accounts of Chemical Research, 2020, 53, 1187-1195.	7.6	100
246	Synthesis and Metalation of Catechol-Functionalized Porous Organic Polymers. Chemistry of Materials, 2012, 24, 1292-1296.	3.2	99
247	G-quadruplex organic frameworks. Nature Chemistry, 2017, 9, 466-472.	6.6	99
248	Porphyrin-Based Thin-Film Molecular Materials with Highly Adjustable Nanoscale Porosity and Permeability Characteristics. Angewandte Chemie - International Edition, 1999, 38, 2222-2224.	7.2	98
249	Rendering High Surface Area, Mesoporous Metal–Organic Frameworks Electronically Conductive. ACS Applied Materials & Interfaces, 2017, 9, 12584-12591.	4.0	98
250	Postsynthetic Incorporation of a Singlet Oxygen Photosensitizer in a Metal–Organic Framework for Fast and Selective Oxidative Detoxification of Sulfur Mustard. Chemistry - A European Journal, 2017, 23, 214-218.	1.7	98
251	Porphyrin sensitized solar cells: TiO2 sensitization with a π-extended porphyrin possessing two anchoring groups. Chemical Communications, 2010, 46, 6090.	2.2	97
252	Determination of specific adsorption of some simple anions at a polycrystalline silver-aqueous interface using differential capacitance and kinetic probe techniques. Journal of Electroanalytical Chemistry and Interfacial Electrochemistry, 1982, 138, 401-423.	0.3	96

#	Article	IF	CITATIONS
253	Structural Diversity of Zirconium Metal–Organic Frameworks and Effect on Adsorption of Toxic Chemicals. Journal of the American Chemical Society, 2020, 142, 21428-21438.	6.6	95
254	Dye Stabilization and Enhanced Photoelectrode Wettability in Water-Based Dye-Sensitized Solar Cells through Post-assembly Atomic Layer Deposition of TiO ₂ . Journal of the American Chemical Society, 2013, 135, 11529-11532.	6.6	94
255	Post metalation of solvothermally grown electroactive porphyrin metal–organic framework thin films. Chemical Communications, 2015, 51, 2414-2417.	2.2	94
256	Beyond the Active Site: Tuning the Activity and Selectivity of a Metal–Organic Framework-Supported Ni Catalyst for Ethylene Dimerization. Journal of the American Chemical Society, 2018, 140, 11174-11178.	6.6	94
257	A mixed dicarboxylate strut approach to enhancing catalytic activity of a de novo urea derivative of metal–organic framework UiO-67. Chemical Communications, 2013, 49, 10920.	2.2	93
258	Detoxification of Chemical Warfare Agents Using a Zr ₆ â€Based Metal–Organic Framework/Polymer Mixture. Chemistry - A European Journal, 2016, 22, 14864-14868.	1.7	93
259	Comparative study of titanium-functionalized UiO-66: support effect on the oxidation of cyclohexene using hydrogen peroxide. Catalysis Science and Technology, 2015, 5, 4444-4451.	2.1	92
260	Redox-Mediator-Assisted Electrocatalytic Hydrogen Evolution from Water by a Molybdenum Sulfide-Functionalized Metal–Organic Framework. ACS Catalysis, 2018, 8, 9848-9858.	5.5	91
261	Separating Solids: Purification of Metal-Organic Framework Materials. Journal of the American Chemical Society, 2008, 130, 8598-8599.	6.6	89
262	Comparison of Interfacial Electron Transfer through Carboxylate and Phosphonate Anchoring Groupsâ€. Journal of Physical Chemistry A, 2007, 111, 6832-6842.	1.1	88
263	Ligand-elaboration as a strategy for engendering structural diversity in porous metal–organic framework compounds. Chemical Communications, 2008, , 3672.	2.2	88
264	Toward Metal–Organic Framework-Based Solar Cells: Enhancing Directional Exciton Transport by Collapsing Three-Dimensional Film Structures. ACS Applied Materials & Interfaces, 2016, 8, 30863-30870.	4.0	88
265	Sinterâ€Resistant Platinum Catalyst Supported by Metal–Organic Framework. Angewandte Chemie - International Edition, 2018, 57, 909-913.	7.2	88
266	Post-Synthetically Elaborated BODIPY-Based Porous Organic Polymers (POPs) for the Photochemical Detoxification of a Sulfur Mustard Simulant. Journal of the American Chemical Society, 2020, 142, 18554-18564.	6.6	88
267	Mesoporous Thin Films of "Molecular Squares―as Sensors for Volatile Organic Compounds. Langmuir, 2000, 16, 3964-3970.	1.6	86
268	Stable Metal–Organic Framework-Supported Niobium Catalysts. Inorganic Chemistry, 2016, 55, 11954-11961.	1.9	85
269	Synthetic Access to Atomically Dispersed Metals in Metal–Organic Frameworks via a Combined Atomic-Layer-Deposition-in-MOF and Metal-Exchange Approach. Chemistry of Materials, 2016, 28, 1213-1219.	3.2	85
270	One Step Backward Is Two Steps Forward: Enhancing the Hydrolysis Rate of UiO-66 by Decreasing [OH [–]]. ACS Catalysis, 2015, 5, 4637-4642.	5.5	84

#	Article	IF	CITATIONS
271	A thermodynamic tank model for studying the effect of higher hydrocarbons on natural gas storage in metal–organic frameworks. Energy and Environmental Science, 2015, 8, 1501-1510.	15.6	84
272	A New Class of Mixed-Valence Systems with Orbitally Degenerate Organic Redox Centers. Examples Based on Hexa-Rhenium Molecular Prisms. Journal of the American Chemical Society, 2006, 128, 12592-12593.	6.6	83
273	Synthesis and Gas Sorption Properties of a Metal-Azolium Framework (MAF) Material. Inorganic Chemistry, 2009, 48, 9971-9973.	1.9	83
274	Electrochemically addressable trisradical rotaxanes organized within a metal–organic framework. Proceedings of the National Academy of Sciences of the United States of America, 2015, 112, 11161-11168.	3.3	83
275	Thermal Stabilization of Metal–Organic Framework-Derived Single-Site Catalytic Clusters through Nanocasting. Journal of the American Chemical Society, 2016, 138, 2739-2748.	6.6	83
276	Surface intervalence enhanced Raman scattering from ferrocyanide on colloidal titanium dioxide. A mode-by-mode description of the Franck-Condon barrier to interfacial charge transfer. Journal of the American Chemical Society, 1991, 113, 1060-1062.	6.6	82
277	Interfacial Charge Transfer and Colloidal Semiconductor Dye-Sensitization:Â Mechanism Assessment via Stark Emission Spectroscopy. Journal of Physical Chemistry B, 2002, 106, 5139-5142.	1.2	81
278	Intervalence enhanced Raman scattering from (NC)5Ru-CN-Ru(NH3)51 A mode-by-mode assessment of the Franck-Condon barrier to intramolecular electron transfer. Journal of the American Chemical Society, 1989, 111, 1142-1144.	6.6	80
279	Room Temperature Synthesis of an 8-Connected Zr-Based Metal–Organic Framework for Top-Down Nanoparticle Encapsulation. Chemistry of Materials, 2018, 30, 2193-2197.	3.2	80
280	A metal–organic framework immobilised iridium pincer complex. Chemical Science, 2016, 7, 4980-4984.	3.7	78
281	Regioselective Atomic Layer Deposition in Metal–Organic Frameworks Directed by Dispersion Interactions. Journal of the American Chemical Society, 2016, 138, 13513-13516.	6.6	78
282	Computationally Guided Discovery of a Catalytic Cobalt-Decorated Metal–Organic Framework for Ethylene Dimerization. Journal of Physical Chemistry C, 2016, 120, 23576-23583.	1.5	78
283	Enhanced Activity of Heterogeneous Pd(II) Catalysts on Acid-Functionalized Metal–Organic Frameworks. ACS Catalysis, 2019, 9, 5383-5390.	5.5	77
284	Does Marcus-Hush theory really work? Optical studies of intervalence transfer in acetylene-bridged biferrocene monocation at infinite dilution and at finite ionic strengths. The Journal of Physical Chemistry, 1990, 94, 1788-1793.	2.9	76
285	Synthesis, Characterization, and Preliminary Intramolecular Energy Transfer Studies of Rigid, Emissive, Rhenium-Linked Porphyrin Dimers. Inorganic Chemistry, 2002, 41, 619-621.	1.9	76
286	Fast Transporting ZnO–TiO ₂ Coaxial Photoanodes for Dye-Sensitized Solar Cells Based on ALD-Modified SiO ₂ Aerogel Frameworks. ACS Nano, 2012, 6, 6185-6196.	7.3	76
287	Systematic Modulation of Quantum (Electron) Tunneling Behavior by Atomic Layer Deposition on Nanoparticulate SnO ₂ and TiO ₂ Photoanodes. Journal of the American Chemical Society, 2013, 135, 16328-16331.	6.6	76
288	Catalytic Solvolytic and Hydrolytic Degradation of Toxic Methyl Paraoxon with La(catecholate)-Functionalized Porous Organic Polymers. ACS Catalysis, 2013, 3, 1454-1459.	5.5	76

#	Article	IF	CITATIONS
289	Isoreticular Series of (3,24)-Connected Metal–Organic Frameworks: Facile Synthesis and High Methane Uptake Properties. Chemistry of Materials, 2014, 26, 1912-1917.	3.2	76
290	Photodriven hydrogen evolution by molecular catalysts using Al ₂ O ₃ -protected perylene-3,4-dicarboximide on NiO electrodes. Chemical Science, 2017, 8, 541-549.	3.7	76
291	Does Marcus-Hush theory really work? The solvent dependence of intervalence charge-transfer infinite dilution. The Journal of Physical Chemistry, 1993, 97, 3278-3282.	2.9	75
292	Coordinative Self-Assembly and Solution-Phase X-ray Structural Characterization of Cavity-Tailored Porphyrin Boxes. Journal of the American Chemical Society, 2008, 130, 836-838.	6.6	75
293	Accessing functionalized porous aromatic frameworks (PAFs) through a de novo approach. CrystEngComm, 2013, 15, 1515-1519.	1.3	75
294	Bridging Zirconia Nodes within a Metal–Organic Framework via Catalytic Ni-Hydroxo Clusters to Form Heterobimetallic Nanowires. Journal of the American Chemical Society, 2017, 139, 10410-10418.	6.6	74
295	Pushing the Limits on Metal–Organic Frameworks as a Catalyst Support: NU-1000 Supported Tungsten Catalysts for <i>o</i> -Xylene Isomerization and Disproportionation. Journal of the American Chemical Society, 2018, 140, 8535-8543.	6.6	73
296	Tetra-Rhenium Molecular Rectangles as Organizational Motifs for the Investigation of Ligand-Centered Mixed Valency:A Three Examples of Full Delocalization. Journal of the American Chemical Society, 2004, 126, 16814-16819.	6.6	71
297	Anisotropic Redox Conductivity within a Metal–Organic Framework Material. Journal of the American Chemical Society, 2019, 141, 17696-17702.	6.6	71
298	Thermally Activated, Inverted Interfacial Electron Transfer Kinetics:Â High Driving Force Reactions between Tin Oxide Nanoparticles and Electrostatically-Bound Molecular Reactants. Journal of the American Chemical Society, 2000, 122, 10956-10963.	6.6	70
299	Optimizing Toxic Chemical Removal through Defectâ€Induced UiOâ€66â€NH ₂ Metal–Organic Framework. Chemistry - A European Journal, 2017, 23, 15913-15916.	1.7	70
300	Strategies for Characterization of Large-Pore Metal-Organic Frameworks by Combined Experimental and Computational Methods. Chemistry of Materials, 2009, 21, 4768-4777.	3.2	68
301	Introducing Nonstructural Ligands to Zirconia-like Metal–Organic Framework Nodes To Tune the Activity of Node-Supported Nickel Catalysts for Ethylene Hydrogenation. ACS Catalysis, 2019, 9, 3198-3207.	5.5	68
302	Unexpected "Spontaneous―Evolution of Catalytic, MOF-Supported Single Cu(II) Cations to Catalytic, MOF-Supported Cu(0) Nanoparticles. Journal of the American Chemical Society, 2020, 142, 21169-21177.	6.6	68
303	Electroabsorption Studies of Intervalence Charge Transfer in (NC)5FeCNOs(NH3)5∹  Experimental Assessment of Charge-Transfer Distance, Solvent Reorganization, and Electronic Coupling Parameters. The Journal of Physical Chemistry, 1996, 100, 15637-15639.	2.9	67
304	Prediction of electron-transfer reactivities from contemporary theory: unified comparisons for electrochemical and homogeneous reactions. The Journal of Physical Chemistry, 1985, 89, 2795-2804.	2.9	66
305	A Porous Multilayer Dye-Based Photoelectrochemical Cell That Unexpectedly Runs in Reverse. Journal of Physical Chemistry B, 2004, 108, 4111-4115.	1.2	66
306	Hematite-based Photo-oxidation of Water Using Transparent Distributed Current Collectors. ACS Applied Materials & Interfaces, 2013, 5, 360-367.	4.0	66

#	Article	IF	CITATIONS
307	Addressing the characterisation challenge to understand catalysis in MOFs: the case of nanoscale Cu supported in NU-1000. Faraday Discussions, 2017, 201, 337-350.	1.6	66
308	Highly Active NiO Photocathodes for H ₂ O ₂ Production Enabled via Outer-Sphere Electron Transfer. Journal of the American Chemical Society, 2018, 140, 4079-4084.	6.6	66
309	Synthesis, linear extinction, and preliminary resonant hyper-Rayleigh scattering studies of gold-core/silver-shell nanoparticles: comparisons of theory and experiment. Chemical Physics Letters, 2002, 352, 421-428.	1.2	65
310	Aromatizing Olefin Metathesis by Ligand Isolation inside a Metal– Organic Framework. Journal of the American Chemical Society, 2013, 135, 14916-14919.	6.6	65
311	Computational Screening of Nanoporous Materials for Hexane and Heptane Isomer Separation. Chemistry of Materials, 2017, 29, 6315-6328.	3.2	65
312	Large-Scale Resonance Amplification of Optical Sensing of Volatile Compounds with Chemoresponsive Visible-Region Diffraction Gratings. Journal of the American Chemical Society, 2002, 124, 6767-6774.	6.6	64
313	Porosity tuning of carborane-based metal–organic frameworks (MOFs) via coordination chemistry and ligand design. Inorganica Chimica Acta, 2010, 364, 266-271.	1.2	64
314	Electroabsorption spectroscopy of molecular inorganic compounds. International Reviews in Physical Chemistry, 1998, 17, 307-329.	0.9	63
315	Atomistic Approach toward Selective Photocatalytic Oxidation of a Mustard-Gas Simulant: A Case Study with Heavy-Chalcogen-Containing PCN-57 Analogues. ACS Applied Materials & Interfaces, 2017, 9, 19535-19540.	4.0	63
316	Surface-enhanced raman spectroscopy of electrochemically characterized interfaces. Journal of Electroanalytical Chemistry and Interfacial Electrochemistry, 1984, 160, 321-333.	0.3	62
317	pH-Dependent Electron Transfer from Re-bipyridyl Complexes to Metal Oxide Nanocrystalline Thin Films. Journal of Physical Chemistry B, 2005, 109, 19345-19355.	1.2	62
318	[Bis(catechol)salen]Mn ^{III} Coordination Polymers as Supportâ€Free Heterogeneous Asymmetric Catalysts for Epoxidation. European Journal of Inorganic Chemistry, 2007, 2007, 4863-4867.	1.0	62
319	A catalytically active vanadyl(catecholate)-decorated metal organic framework via post-synthesis modifications. CrystEngComm, 2012, 14, 4115.	1.3	62
320	Photochemical Quartz Crystal Microbalance Study of the Nanocrystalline Titanium Dioxide Semiconductor Electrode/Water Interface:Â Simultaneous Photoaccumulation of Electrons and Protons. The Journal of Physical Chemistry, 1996, 100, 14578-14580.	2.9	61
321	Rapid derivatization of mesoporous thin-film materials based on Re(I) zinc-porphyrin â€~molecular squares': selective modification of mesopore size and shape by binding of aromatic nitrogen donor ligands. Coordination Chemistry Reviews, 1999, 190-192, 29-45.	9.5	61
322	Complete Double Epoxidation of Divinylbenzene Using Mn(porphyrin)-Based Porous Organic Polymers. ACS Catalysis, 2015, 5, 4859-4866.	5.5	61
323	Amorphous TiO ₂ Compact Layers via ALD for Planar Halide Perovskite Photovoltaics. ACS Applied Materials & Interfaces, 2016, 8, 24310-24314.	4.0	61
324	Modulating the rate of charge transport in a metal–organic framework thin film using host:guest chemistry. Chemical Communications, 2016, 52, 1705-1708.	2.2	61

#	Article	IF	CITATIONS
325	From 2-methylimidazole to 1,2,3-triazole: a topological transformation of ZIF-8 and ZIF-67 by post-synthetic modification. Chemical Communications, 2017, 53, 2028-2031.	2.2	61
326	In Search of the Inverted Region:Â Chromophore-Based Driving Force Dependence of Interfacial Electron Transfer Reactivity at the Nanocrystalline Titanium Dioxide Semiconductor/Solution Interfaceâ€. Journal of Physical Chemistry B, 2000, 104, 10871-10877.	1.2	60
327	Experimental Studies of Light-Induced Charge Transfer and Charge Redistribution in (X2-Bipyridine)ReI(CO)3Cl Complexes. Inorganic Chemistry, 2002, 41, 2909-2919.	1.9	60
328	Stable and catalytically active iron porphyrin-based porous organic polymer: Activity as both a redox and Lewis acid catalyst. Scientific Reports, 2015, 5, 10621.	1.6	60
329	Preresonance Raman studies of metal-to-ligand charge transfer in (NH3)4Ru(2,2'-bipyridine)2+. In situ bond length changes, force constants, and reorganization energies. Journal of the American Chemical Society, 1989, 111, 4704-4712.	6.6	59
330	Resonance Raman studies in the extended near infrared region: experimental verification of a three-site mixing mechanism for valence delocalization in the Creutz-Taube ion. Journal of the American Chemical Society, 1994, 116, 2171-2172.	6.6	59
331	Electroabsorption Studies of Metal-to-Ligand Charge Transfer in Ru(phenanthroline)32+:Â Evidence for Intrinsic Charge Localization in the Initially Formed Excited State. Inorganic Chemistry, 1997, 36, 3318-3321.	1.9	59
332	Large Electron Transfer Rate Effects from the Duschinsky Mixing of Vibrations. Journal of Physical Chemistry A, 2001, 105, 5317-5325.	1.1	59
333	Amphiphilic Porphyrin Nanocrystals: Morphology Tuning and Hierarchical Assembly. Advanced Materials, 2008, 20, 3543-3549.	11.1	59
334	Computational Modeling of Plasmon-Enhanced Light Absorption in a Multicomponent Dye Sensitized Solar Cell. Journal of Physical Chemistry C, 2012, 116, 10215-10221.	1.5	59
335	Real-Time Observation of Atomic Layer Deposition Inhibition: Metal Oxide Growth on Self-Assembled Alkanethiols. ACS Applied Materials & Interfaces, 2014, 6, 11891-11898.	4.0	59
336	Adding to the Arsenal of Zirconiumâ€Based Metal–Organic Frameworks: <i>the</i> Topology as a Platform for Solventâ€Assisted Metal Incorporation. European Journal of Inorganic Chemistry, 2016, 2016, 4349-4352.	1.0	59
337	Improvement of Methane–Framework Interaction by Controlling Pore Size and Functionality of Pillared MOFs. Inorganic Chemistry, 2017, 56, 2581-2588.	1.9	59
338	Tuning ethylene gas adsorption via metal node modulation: Cu-MOF-74 for a high ethylene deliverable capacity. Chemical Communications, 2017, 53, 9376-9379.	2.2	59
339	Energy relationships in optical and thermal electron transfer. Temperature dependence of an intervalence transfer absorption band. The Journal of Physical Chemistry, 1992, 96, 10820-10830.	2.9	58
340	Functionalized Defects through Solvent-Assisted Linker Exchange: Synthesis, Characterization, and Partial Postsynthesis Elaboration of a Metal–Organic Framework Containing Free Carboxylic Acid Moieties. Inorganic Chemistry, 2015, 54, 1785-1790.	1.9	58
341	Generalized synthesis of cis- and trans-dioxorhenium(V) (bi)pyridyl complexes. Inorganic Chemistry, 1991, 30, 130-133.	1.9	57
342	Greenlighting Photoelectrochemical Oxidation of Water by Iron Oxide. ACS Nano, 2014, 8, 12199-12207.	7.3	57

#	Article	IF	CITATIONS
343	A visually detectable pH responsive zirconium metal–organic framework. Chemical Communications, 2016, 52, 3438-3441.	2.2	57
344	Installing Heterobimetallic Cobalt–Aluminum Single Sites on a Metal Organic Framework Support. Chemistry of Materials, 2016, 28, 6753-6762.	3.2	56
345	Efficient extraction of sulfate from water using a Zr-metal–organic framework. Dalton Transactions, 2016, 45, 93-97.	1.6	56
346	Metal–Organic Framework Supported Single Site Chromium(III) Catalyst for Ethylene Oligomerization at Low Pressure and Temperature. ACS Sustainable Chemistry and Engineering, 2019, 7, 2553-2557.	3.2	56
347	Enhanced activity of enantioselective (salen)Mn(III) epoxidation catalysts through supramolecular complexation. Journal of Molecular Catalysis A, 2001, 174, 15-20.	4.8	55
348	Enhanced Electrocatalytic Reduction of CO ₂ with Ternary Ni-Fe ₄ S ₄ and Co-Fe ₄ S ₄ -Based Biomimetic Chalcogels. Journal of the American Chemical Society, 2011, 133, 15854-15857.	6.6	55
349	Experimental estimate of the electron-tunneling distance for some outer-sphere electrochemical reactions. The Journal of Physical Chemistry, 1984, 88, 1463-1467.	2.9	54
350	Synthesis and preliminary photophysical studies of intramolecular electron transfer in crown-linked donor- (chromophore-) acceptor complexes. Inorganic Chemistry, 1992, 31, 3192-3194.	1.9	54
351	Interfacial Charge-Transfer Pathways:Â Evidence for Marcus-Type Inverted Electron Transfer in Metal Oxide Semiconductor/Inorganic Dye Systems. Journal of the American Chemical Society, 1999, 121, 8399-8400.	6.6	54
352	Post-assembly transformations of porphyrin-containing metal–organic framework (MOF) films fabricated via automated layer-by-layer coordination. Chemical Communications, 2015, 51, 85-88.	2.2	54
353	Effect of Cation Rotation on Charge Dynamics in Hybrid Lead Halide Perovskites. Journal of Physical Chemistry C, 2016, 120, 16577-16585.	1.5	54
354	Inorganic "Conductive Glass―Approach to Rendering Mesoporous Metal–Organic Frameworks Electronically Conductive and Chemically Responsive. ACS Applied Materials & Interfaces, 2018, 10, 30532-30540.	4.0	54
355	Electrochemical assembly of metallopolymeric films via reduction of coordinated 5-chlorophenanthroline. Inorganic Chemistry, 1989, 28, 1533-1537.	1.9	53
356	From Layered Structures to Cubic Frameworks: Expanding the Structural Diversity of Uranyl Carboxyphosphonates via the Incorporation of Cobalt. Crystal Growth and Design, 2011, 11, 1385-1393.	1.4	53
357	Thermally Enhancing the Surface Areas of Yamamoto-Derived Porous Organic Polymers. Chemistry of Materials, 2013, 25, 12-16.	3.2	53
358	Enhanced activity of manganese(III) porphyrin epoxidation catalysts through supramolecular complexation. Journal of Molecular Catalysis A, 2000, 156, 79-84.	4.8	52
359	Intervalence excitation of the Creutz-Taube ion. Resonance Raman and time-dependent scattering studies of Franck-Condon effects. Chemical Physics Letters, 1995, 235, 521-527.	1.2	51
360	Dye-Sensitized Solar Cells: Sensitizer-Dependent Injection into ZnO Nanotube Electrodes. Langmuir, 2010, 26, 1401-1404.	1.6	51

#	Article	IF	CITATIONS
361	Stabilizing unstable species through single-site isolation: a catalytically active TaV trialkyl in a porous organic polymer. Chemical Science, 2013, 4, 2483.	3.7	51
362	Detection of chemical species using ultraviolet microdisk lasers. Applied Physics Letters, 2004, 85, 3666-3668.	1.5	50
363	Understanding excess uptake maxima for hydrogen adsorption isotherms in frameworks with rht topology. Chemical Communications, 2012, 48, 10496.	2.2	50
364	Supramolecular chemistry: Functional structures on the mesoscale. Proceedings of the National Academy of Sciences of the United States of America, 2001, 98, 11849-11850.	3.3	49
365	Selective Solvent-Assisted Linker Exchange (SALE) in a Series of Zeolitic Imidazolate Frameworks. Inorganic Chemistry, 2015, 54, 7142-7144.	1.9	49
366	Experimental assessment of dynamic structural parameters for homogeneous and interfacial charge-transfer reactions: case studies based on time-dependent Raman scattering methods. Electrochimica Acta, 1991, 36, 1775-1785.	2.6	48
367	Distance-Engineered Plasmon-Enhanced Light Harvesting in CdSe Quantum Dots. Journal of Physical Chemistry Letters, 2013, 4, 3527-3533.	2.1	48
368	An effective strategy for creating asymmetric MOFs for chirality induction: a chiral Zr-based MOF for enantioselective epoxidation. Catalysis Science and Technology, 2019, 9, 3388-3397.	2.1	48
369	Solvent control of oxidation state distribution and electronic delocalization in an osmium-ruthenium, mixed-metal dimer. Journal of the American Chemical Society, 1986, 108, 5349-5350.	6.6	47
370	Aspects of Intervalence Charge Transfer in Cyanide-Bridged Systems:  Modulated Electric Field Assessment of Distances, Polarizability Changes, and Anticipated First Hyperpolarizability Characteristics. Journal of Physical Chemistry A, 1998, 102, 8320-8324.	1.1	47
371	Solution-Phase Structural Characterization of Supramolecular Assemblies by Molecular Diffraction. Journal of the American Chemical Society, 2007, 129, 1578-1585.	6.6	47
372	Two Azolium Rings Are Better Than One: A Strategy for Controlling Catenation and Morphology in Zn and Cu Metal–Organic Frameworks. Crystal Growth and Design, 2011, 11, 4747-4750.	1.4	47
373	Stabilization of a highly porous metal–organic framework utilizing a carborane-based linker. Chemical Communications, 2015, 51, 6521-6523.	2.2	47
374	Pore-Templated Growth of Catalytically Active Gold Nanoparticles within a Metal–Organic Framework. Chemistry of Materials, 2019, 31, 1485-1490.	3.2	47
375	Electrochemical Quartz Crystal Microbalance Studies of Electron Addition at Nanocrystalline Tin Oxide/Water and Zinc Oxide/Water Interfaces:Â Evidence for Band-Edge-Determining Proton Uptake. Journal of Physical Chemistry B, 1997, 101, 2426-2429.	1.2	46
376	EQCM Investigations of Dye-Functionalized Nanocrystalline Titanium Dioxide Electrode/Solution Interfaces:  Does Luminescence Report Directly on Interfacial Electron Transfer Kinetics?. Journal of Physical Chemistry B, 1999, 103, 3797-3799.	1.2	46
377	High propylene/propane adsorption selectivity in a copper(catecholate)-decorated porous organic polymer. Journal of Materials Chemistry A, 2014, 2, 299-302.	5.2	46
378	Proton Conducting Self-Assembled Metal–Organic Framework/Polyelectrolyte Hollow Hybrid Nanostructures. ACS Applied Materials & Interfaces, 2016, 8, 23015-23021.	4.0	46

#	Article	IF	CITATIONS
379	Photodriven Oxidation of Surface-Bound Iridium-Based Molecular Water-Oxidation Catalysts on Perylene-3,4-dicarboximide-Sensitized TiO ₂ Electrodes Protected by an Al ₂ O ₃ Layer. Journal of Physical Chemistry C, 2017, 121, 3752-3764.	1.5	46
380	Thermal Conductivity of ZIF-8 Thin-Film under Ambient Gas Pressure. ACS Applied Materials & Interfaces, 2017, 9, 28139-28143.	4.0	46
381	Permeable Nonaggregating Porphyrin Thin Films That Display Enhanced Photophysical Properties. Langmuir, 2004, 20, 10560-10566.	1.6	45
382	Catalytically active supramolecular porphyrin boxes: acceleration of the methanolysis of phosphate triesters via a combination of increased local nucleophilicity and reactant encapsulation. Chemical Science, 2012, 3, 1938.	3.7	45
383	A MOF platform for incorporation of complementary organic motifs for CO ₂ binding. Chemical Communications, 2015, 51, 12478-12481.	2.2	45
384	Atomic Layer Deposition of Ultrathin Nickel Sulfide Films and Preliminary Assessment of Their Performance as Hydrogen Evolution Catalysts. Langmuir, 2016, 32, 12005-12012.	1.6	45
385	One Electron Changes Everything. A Multispecies Copper Redox Shuttle for Dye-Sensitized Solar Cells. Journal of Physical Chemistry C, 2016, 120, 3731-3740.	1.5	45
386	Atomic Layer Deposition in a Metal–Organic Framework: Synthesis, Characterization, and Performance of a Solid Acid. Chemistry of Materials, 2017, 29, 1058-1068.	3.2	45
387	Rhenium-Linked Multiporphyrin Assemblies:Synthesis and Properties. , 0, , 145-165.		44
388	Layer-by-Layer Assembled Films of Perylene Diimide- and Squaraine-Containing Metal–Organic Framework-like Materials: Solar Energy Capture and Directional Energy Transfer. ACS Applied Materials & Interfaces, 2016, 8, 24983-24988.	4.0	44
389	Design and Synthesis of a Water‣table Anionic Uraniumâ€Based Metal–Organic Framework (MOF) with Ultra Large Pores. Angewandte Chemie, 2016, 128, 10514-10518.	1.6	44
390	Site-Directed Synthesis of Cobalt Oxide Clusters in a Metal–Organic Framework. ACS Applied Materials & Interfaces, 2018, 10, 15073-15078.	4.0	44
391	Electrochemical and homogeneous exchange kinetics for transition-metal aqua couples: anomalous behavior of hexaaquairon(III/II). Inorganic Chemistry, 1983, 22, 2557-2564.	1.9	43
392	Scanning Electrochemical Microscopy Assessment of Rates of Molecular Transport through Mesoporous Thin-Films of Porphyrinic "Molecular Squares― Journal of Physical Chemistry B, 2001, 105, 8944-8950.	1.2	43
393	Micropatterned Polymeric Gratings as Chemoresponsive Volatile Organic Compound Sensors: Implications for Analyte Detection and Identification via Diffraction-Based Sensor Arrays. Analytical Chemistry, 2003, 75, 2392-2398.	3.2	43
394	Effective Panchromatic Sensitization of Electrochemical Solar Cells: Strategy and Organizational Rules for Spatial Separation of Complementary Light Harvesters on High-Area Photoelectrodes. Journal of the American Chemical Society, 2012, 134, 19820-19827.	6.6	43
395	Design, Synthesis, Characterization, and Catalytic Properties of a Large-Pore Metal-Organic Framework Possessing Single-Site Vanadyl(monocatecholate) Moieties. Crystal Growth and Design, 2013, 13, 3528-3534.	1.4	43
396	Post-Assembly Atomic Layer Deposition of Ultrathin Metal-Oxide Coatings Enhances the Performance of an Organic Dye-Sensitized Solar Cell by Suppressing Dye Aggregation. ACS Applied Materials & Interfaces, 2015, 7, 5150-5159.	4.0	43

#	Article	IF	CITATIONS
397	Postassembly Transformation of a Catalytically Active Composite Material, Pt@ZIF-8, via Solvent-Assisted Linker Exchange. Inorganic Chemistry, 2016, 55, 1361-1363.	1.9	43
398	Bifunctional Porphyrin-Based Nano-Metal–Organic Frameworks: Catalytic and Chemosensing Studies. Inorganic Chemistry, 2018, 57, 3855-3864.	1.9	43
399	Probing the molecular basis of solvent reorganization in electron-transfer reactions. The Journal of Physical Chemistry, 1988, 92, 2817-2820.	2.9	42
400	Electrochemical variational study of donor/acceptor orbital mixing and electronic coupling in cyanide-bridged mixed-valence complexes. Inorganic Chemistry, 1992, 31, 3170-3172.	1.9	42
401	Borderline Class II/III Ligand-Centered Mixed Valency in a Porphyrinic Molecular Rectangle. Inorganic Chemistry, 2005, 44, 5789-5797.	1.9	42
402	Intramolecular Energy and Electron Transfer within a Diazaperopyrenium-Based Cyclophane. Journal of the American Chemical Society, 2017, 139, 4107-4116.	6.6	42
403	Crystal to Crystal Guest Exchange in a Mixed Ligand Metalâ^'Organic Framework. Crystal Growth and Design, 2009, 9, 4588-4591.	1.4	41
404	Solvent-Induced Electron Transfer and Delocalization in Mixed-Valence Complexes. Electrochemistry. Journal of the American Chemical Society, 1996, 118, 3724-3729.	6.6	40
405	Solvent Control of Vibronic Coupling upon Intervalence Charge Transfer Excitation of (CN)5FeCNRu(NH3)5- as Revealed by Resonance Raman and Near-Infrared Absorption Spectroscopies. Journal of the American Chemical Society, 1998, 120, 5848-5849.	6.6	40
406	Supramolecular porphyrinic prisms: coordinative assembly and solution phase X-ray structural characterization. Chemical Communications, 2006, , 4581.	2.2	40
407	Insights into the Structure–Activity Relationships in Metal–Organic Framework-Supported Nickel Catalysts for Ethylene Hydrogenation. ACS Catalysis, 2020, 10, 8995-9005.	5.5	40
408	Light-Harvesting "Antenna―Behavior in NU-1000. ACS Energy Letters, 2021, 6, 848-853.	8.8	40
409	The driving-force dependence of electrochemical rate parameters: origins of anodic-cathodic asymmetries for metal-aquo redox couples. The Journal of Physical Chemistry, 1984, 88, 6128-6135.	2.9	39
410	Analysis of Molecular Square Size and Purity via Pulsed-Field Gradient NMR Spectroscopy. Inorganic Chemistry, 2002, 41, 6172-6174.	1.9	39
411	Enhanced catalytic decomposition of a phosphate triester by modularly accessible bimetallic porphyrin dyads and dimers. Chemical Communications, 2012, 48, 4178.	2.2	39
412	Removal of airborne toxic chemicals by porous organic polymers containing metal–catecholates. Chemical Communications, 2013, 49, 2995.	2.2	39
413	Metal–Organic-Framework-Supported and -Isolated Ceria Clusters with Mixed Oxidation States. ACS Applied Materials & Interfaces, 2019, 11, 47822-47829.	4.0	39
414	SiO2 Aerogel Templated, Porous TiO2 Photoanodes for Enhanced Performance in Dye-Sensitized Solar Cells Containing a Ni(III)/(IV) Bis(dicarbollide) Shuttle. Journal of Physical Chemistry C, 2011, 115, 11257-11264.	1.5	38

#	Article	IF	CITATIONS
415	Size effect of the active sites in UiO-66-supported nickel catalysts synthesized via atomic layer deposition for ethylene hydrogenation. Inorganic Chemistry Frontiers, 2017, 4, 820-824.	3.0	38
416	Reactive Porous Polymers for Detoxification of a Chemical Warfare Agent Simulant. Chemistry of Materials, 2020, 32, 9299-9306.	3.2	38
417	Noncontinuum solvent effects upon the intrinsic free-energy barrier for electron-transfer reactions. The Journal of Physical Chemistry, 1985, 89, 1601-1608.	2.9	37
418	Solvent control of orbital mixing and electronic coupling in ligand-bridged mixed-valence complexes: evidence for an intervalence hole-transfer pathway. Journal of the American Chemical Society, 1990, 112, 1563-1565.	6.6	37
419	Comparative absorption, electroabsorption and electrochemical studies of intervalence electron transfer and electronic coupling in cyanide-bridged bimetallic systems: ancillary ligand effects. Chemical Physics, 2000, 253, 313-322.	0.9	37
420	Organic Photovoltaics Interdigitated on the Molecular Scale. Journal of the Electrochemical Society, 2006, 153, A527.	1.3	37
421	Pt@ZIF-8 composite for the regioselective hydrogenation of terminal unsaturations in 1,3-dienes and alkynes. Inorganic Chemistry Frontiers, 2015, 2, 448-452.	3.0	37
422	The ferrocene assumption in redox thermodynamics: implications from optical intervalence studies of ion pairing to ferrocenium. Inorganic Chemistry, 1990, 29, 5010-5012.	1.9	36
423	High-Valent Oxo, Methoxorhenium Complexes: Models for Intermediates and Transition States in Proton-Coupled Multi-Electron Transfer Reactions. Journal of the American Chemical Society, 1995, 117, 1411-1421.	6.6	36
424	Primitive Molecular Recognition Effects in Electron Transfer Processes:Â Modulation of ((Trimethylammonio)methyl)ferrocenium/ferrocene Self-Exchange Kinetics via Hydrophobic Encapsulation. Inorganic Chemistry, 1996, 35, 970-973.	1.9	36
425	Development and application of patterned conducting polymer thin films as chemoresponsive and electrochemically responsive optical diffraction gratings. Journal of Electroanalytical Chemistry, 2001, 500, 185-191.	1.9	36
426	Ammonia Capture within Zirconium Metal–Organic Frameworks: Reversible and Irreversible Uptake. ACS Applied Materials & Interfaces, 2021, 13, 20081-20093.	4.0	36
427	Optical electron transfer in mixed solvents. Major energetic effects from unsymmetrical secondary coordination. Inorganic Chemistry, 1987, 26, 2657-2660.	1.9	35
428	Intervalence transfer in the dimer pentaammine(.mu4,4'-bipyridine)diruthenium(5+). Inorganic Chemistry, 1987, 26, 2332-2334.	1.9	35
429	Walljet Electrochemistry:Â Quantifying Molecular Transport through Metallopolymeric and Zirconium Phosphonate Assembled Porphyrin Square Thin Films. Langmuir, 2004, 20, 4422-4429.	1.6	35
430	C- and Z-Shaped Coordination Compounds. Synthesis, Structure, and Spectroelectrochemistry of cis- and trans-[Re(CO)3(L)]2-2,2'-bisbenzimidizolate with L = 4-Phenylpyridine, 2,4'-Bipyridine, or Pyridine. Inorganic Chemistry, 2005, 44, 8707-8714.	1.9	35
431	Underlying Spinâ [°] Orbit Coupling Structure of Intervalence Charge Transfer Bands in Dinuclear Polypyridyl Complexes of Ruthenium and Osmium. Inorganic Chemistry, 2006, 45, 3261-3274.	1.9	35
432	Intramolecular Electron Transfer in Biferrocene Monocation:  Evaluation of Franckâ^'Condon Effects via a Time-Dependent Analysis of Resonance Raman Scattering in the Extended Near-Infrared. Journal of Physical Chemistry A, 1997, 101, 8070-8076.	1.1	34

#	Article	IF	CITATIONS
433	Fast energy transfer within a self-assembled cyclic porphyrin tetramer. Chemical Communications, 2008, , 1886.	2.2	34
434	Effects of Adsorbed Pyridine Derivatives and Ultrathin Atomic-Layer-Deposited Alumina Coatings on the Conduction Band-Edge Energy of TiO ₂ and on Redox-Shuttle-Derived Dark Currents. Langmuir, 2013, 29, 806-814.	1.6	34
435	Chemoselective Hydrogenation of Crotonaldehyde Catalyzed by an Au@ZIFâ€8 Composite. ChemCatChem, 2016, 8, 855-860.	1.8	34
436	Photon Upconversion in a Glowing Metal–Organic Framework. Journal of the American Chemical Society, 2021, 143, 5053-5059.	6.6	34
437	An Electrically Conductive Tetrathiafulvalene-Based Hydrogen-Bonded Organic Framework. , 2022, 4, 128-135.		34
438	Thermochromic effects in an asymmetric mixed-valence system. Inorganic Chemistry, 1992, 31, 3322-3324.	1.9	33
439	Electrochemical and spectral probes of metal/ligand orbital mixing in tetraammine(bipyridine)ruthenium(2+) and tetrammine(phenanthroline)ruthenium(2+). Inorganic Chemistry, 1992, 31, 125-128.	1.9	33
440	Hollow porphyrin prisms: modular formation of permanent, torsionally rigid nanostructures via templated olefin metathesis. Chemical Communications, 2008, , 3375.	2.2	33
441	Introducing Perovskite Solar Cells to Undergraduates. Journal of Physical Chemistry Letters, 2015, 6, 251-255.	2.1	33
442	Boosting Transport Distances for Molecular Excitons within Photoexcited Metal–Organic Framework Films. ACS Applied Materials & Interfaces, 2018, 10, 34409-34417.	4.0	33
443	Synthesis and electrochemistry of 2,2'-bipyridyl complexes of dioxorhenium(V). Inorganic Chemistry, 1990, 29, 238-244.	1.9	32
444	Energetics of Electron Transfer at the Nanocrystalline Titanium Dioxide Semiconductor/Aqueous Solution Interface:  pH Invariance of the Metal-Based Formal Potential of a Representative Surface-Attached Dye Couple. Journal of Physical Chemistry B, 1997, 101, 1493-1495.	1.2	32
445	Imaging Size-Selective Permeation through Micropatterned Thin Films Using Scanning Electrochemical Microscopy. Analytical Chemistry, 2000, 72, 3122-3128.	3.2	32
446	Permeable, Microporous Polymeric Membrane Materials Constructed from Discrete Molecular Squares. Advanced Materials, 2003, 15, 1936-1939.	11.1	32
447	Ultrathin micropatterned porphyrin films assembled via zirconium phosphonate chemistry. Polyhedron, 2003, 22, 3065-3072.	1.0	32
448	Detoxification of a Mustard-Gas Simulant by Nanosized Porphyrin-Based Metal–Organic Frameworks. ACS Applied Nano Materials, 2019, 2, 465-469.	2.4	32
449	The Synthesis Science of Targeted Vapor-Phase Metal–Organic Framework Postmodification. Journal of the American Chemical Society, 2020, 142, 242-250.	6.6	32
450	Ligand tuning effects upon the multielectron reduction and single-electron oxidation of (bi)pyridyl complexes of cis- and trans-dioxorhenium(V): redox thermodynamics, preliminary electrochemical kinetics, and charge-transfer absorption spectroscopy. Inorganic Chemistry, 1991, 30, 2928-2938.	1.9	31

#	Article	IF	CITATIONS
451	A luminescent tricarbonylchlororhenium(I) complex featuring a flexible "crown etherâ€ligand. Manipulation of photoexcited state properties via binding of small cations â€. Journal of the Chemical Society Dalton Transactions, 1999, , 3407-3411.	1.1	31
452	Mechanism for zirconium oxide atomic layer deposition using bis(methylcyclopentadienyl)methoxymethyl zirconium. Applied Physics Letters, 2007, 91, 253123.	1.5	31
453	Towards artificial enzymes. Nature Chemistry, 2010, 2, 432-433.	6.6	31
454	Two Large-Pore Metal–Organic Frameworks Derived from a Single Polytopic Strut. Crystal Growth and Design, 2012, 12, 1075-1080.	1.4	31
455	Influence of specific reactant-solvent interactions on intrinsic activation entropies for outer-sphere electron-transfer reactions. The Journal of Physical Chemistry, 1984, 88, 1860-1864.	2.9	30
456	Optical electron transfer processes. The dependence of intervalence line shape and transition energy on chromophore concentration. Chemical Physics Letters, 1988, 150, 399-405.	1.2	30
457	Linear free energy relations for multielectron transfer kinetics: a brief look at the Broensted/Tafel analogy. The Journal of Physical Chemistry, 1990, 94, 2378-2380.	2.9	30
458	Solvent-induced and polyether-ligand-induced redox isomerization within an asymmetrically coordinated mixed-valence ion: trans-tetraamminebis(2,2'-bipyridine)(.mu4-cyanopyridine)chloro(pyridine)diruthenium(4+), trans-(py)(NH3)4Ru(4-NCpy)Ru(2,2'-bpy)2Cl4+. Inorganic Chemistry, 1991, 30, 3856-3860.	1.9	30
459	Electronic Structure and Spectroscopy of Cadmium Thiolate Clusters. The Journal of Physical Chemistry, 1996, 100, 12204-12213.	2.9	30
460	Energy Conversion Chemistry: Mechanisms of Charge Transfer at Metal-Oxide Semiconductor/Solution Interfaces. Journal of Chemical Education, 1997, 74, 657.	1.1	30
461	Interrogation of Nanoscale Silicon Dioxide/Water Interfaces via Hyper-Rayleigh Scattering. Journal of Physical Chemistry B, 1998, 102, 1845-1848.	1.2	30
462	A Convenient Route to High Area, Nanoparticulate TiO ₂ Photoelectrodes Suitable for High-Efficiency Energy Conversion in Dye-Sensitized Solar Cells. Langmuir, 2011, 27, 1996-1999.	1.6	30
463	Tuning the properties of metal–organic framework nodes as supports of single-site iridium catalysts: node modification by atomic layer deposition of aluminium. Faraday Discussions, 2017, 201, 195-206.	1.6	30
464	The prediction of electrochemical reactivities from contemporary theory: some comparisons with experiment. Journal of Electroanalytical Chemistry and Interfacial Electrochemistry, 1984, 168, 313-334.	0.3	29
465	Resonance-enhanced Raman scattering in the near-infrared region. Preliminary studies of charge transfer in the symmetric dimers (2,2'-bpy)2ClRu-4,4'-bpy-RuCl(2,2'-bpy)24+/3+/2+, (H3N)5Ru-4,4'-bpy-Ru(NH3)56+/5+/4+, and (NC)5Fe-4,4'-bpy-Fe(CN)54-/5-/6 Journal of the American Chemical Society, 1990, 112, 4999-5002.	6.6	29
466	Crown ether encapsulation effects upon optical electron-transfer energetics in a symmetrical mixed-valence system. Inorganic Chemistry, 1991, 30, 4685-4687.	1.9	29
467	Photoinduced Electron Transfer and Intramolecular Folding in a Tricarbonylrhenium (Bi)pyridine Based Donor/Crown/Acceptor Assembly:Â Dependence on Solvent. Inorganic Chemistry, 1996, 35, 2032-2035.	1.9	29
468	Orbital Specific Charge Transfer Distances, Solvent Reorganization Energies, and Electronic Coupling Energies:Â Electronic Stark Effect Studies of Parallel and Orthogonal Intervalence Transfer in (NC)5Osllâ^'CNâ^'RullI(NH3)5 Journal of the American Chemical Society, 1997, 119, 4070-4073.	6.6	29

#	Article	IF	CITATIONS
469	Anthracene-Induced Turnover Enhancement in the Manganese Porphyrin-Catalyzed Epoxidation of Olefins. Inorganic Chemistry, 2005, 44, 5523-5529.	1.9	29
470	Î ³ -Cyclodextrin Cuprate Sandwich-Type Complexes. Inorganic Chemistry, 2013, 52, 2854-2861.	1.9	29
471	Towards hydroxamic acid linked zirconium metal–organic frameworks. Materials Chemistry Frontiers, 2017, 1, 1194-1199.	3.2	29
472	Vapor-Phase Fabrication and Condensed-Phase Application of a MOF-Node-Supported Iron Thiolate Photocatalyst for Nitrate Conversion to Ammonium. ACS Applied Energy Materials, 2019, 2, 8695-8700.	2.5	29
473	The significance of electrochemical activation parameters for surface-attached reactants. Journal of Electroanalytical Chemistry and Interfacial Electrochemistry, 1983, 145, 43-51.	0.3	28
474	Redox thermodynamics of dinuclear transition-metal complexes. Unusual entropy and electronic coupling effects in mixed solvents. Inorganic Chemistry, 1989, 28, 3791-3795.	1.9	28
475	Molecular structure of (bipyridine)dioxobis(pyridine)rhenium(1+) perchlorate: an unusual example of a d2 metal complex with a cis-dioxo ligand configuration. Inorganic Chemistry, 1990, 29, 1791-1792.	1.9	28
476	A complete experimental assessment of Franck-Condon structural effects for an irreversible outer-sphere electron-transfer reaction: applications of time-dependent Raman scattering theory to the one-electron reduction of 4-cyano-N-methylpyridinium. The Journal of Physical Chemistry, 1991, 95, 10535-10537.	2.9	28
477	Ruthenium ammine/crown ether interactions in solution: effects of modification of both guest and host on the strength of second-sphere complexation. Inorganic Chemistry, 1993, 32, 2001-2004.	1.9	28
478	"Perfect―Electrochemical Molecular Sieving by Thin and Ultrathin Metallopolymeric Films. Langmuir, 1999, 15, 837-843.	1.6	28
479	Threeâ€Dimensional Architectures Incorporating Stereoregular Donor–Acceptor Stacks. Chemistry - A European Journal, 2013, 19, 8457-8465.	1.7	28
480	Metallacarborane-Based Metal–Organic Framework with a Complex Topology. Crystal Growth and Design, 2014, 14, 1324-1330.	1.4	28
481	A dual approach to tuning the porosity of porous organic polymers: controlling the porogen size and supercritical CO ₂ processing. Chemical Science, 2014, 5, 782-787.	3.7	28
482	Fabrication of Transparent-Conducting-Oxide-Coated Inverse Opals as Mesostructured Architectures for Electrocatalysis Applications: A Case Study with NiO. ACS Applied Materials & Interfaces, 2014, 6, 12290-12294.	4.0	28
483	Elucidating the Nanoparticle–Metal Organic Framework Interface of Pt@ZIF-8 Catalysts. Journal of Physical Chemistry C, 2017, 121, 25079-25091.	1.5	28
484	Probing charge transfer characteristics in a donor–acceptor metal–organic framework by Raman spectroelectrochemistry and pressure-dependence studies. Physical Chemistry Chemical Physics, 2018, 20, 25772-25779.	1.3	28
485	Product Inhibition and the Catalytic Destruction of a Nerve Agent Simulant by Zirconium-Based Metal–Organic Frameworks. ACS Applied Materials & Interfaces, 2021, 13, 30565-30575.	4.0	28
486	Solvent-dependent redox thermodynamics of metal amine complexes. Delineation of specific solvation effects. Inorganic Chemistry, 1990, 29, 4322-4328.	1.9	27

#	Article	IF	CITATIONS
487	Modulation of Outer-Sphere Electron Transfer Reactivity via Primitive Molecular Recognition Effects: Ru(NH3)5(4-methyl-pyridine)3+/2+ Self-Exchange Kinetics in the Presence of Macrocyclic Polyether Species. Journal of the American Chemical Society, 1995, 117, 9085-9086.	6.6	27
488	Fabrication of Thin Films of α-Fe ₂ O ₃ via Atomic Layer Deposition Using Iron Bisamidinate and Water under Mild Growth Conditions. ACS Applied Materials & Interfaces, 2015, 7, 16138-16142.	4.0	27
489	MOFs and their grafted analogues: regioselective epoxide ring-opening with Zr ₆ nodes. Catalysis Science and Technology, 2016, 6, 6480-6484.	2.1	27
490	Zirconium Metal–Organic Frameworks Integrating Chloride Ions for Ammonia Capture and/or Chemical Separation. ACS Applied Materials & Interfaces, 2021, 13, 22485-22494.	4.0	27
491	Perturbation of the electronic structure of the Creutz-Taube ion via asymmetric encapsulation with macrocyclic ether species. Journal of the American Chemical Society, 1993, 115, 4379-4380.	6.6	26
492	Intervalence Energy Effects Accompanying Double Crown Encapsulation of the Creutz-Taube Ion: An Interpretation Based on Three-Site Mixing. Inorganic Chemistry, 1994, 33, 4421-4424.	1.9	26
493	Characterization and Purification of Supramolecular Metal Complexes Using Gel-Permeation Chromatography. Inorganic Chemistry, 2004, 43, 2013-2017.	1.9	26
494	The Effective Electron-Transfer Distance in Dinuclear Ruthenium Complexes Containing the Unsymmetrical Bridging Ligand 3,5-Bis(2-pyridyl)-1,2,4-triazolate. European Journal of Inorganic Chemistry, 2006, 2006, 772-783.	1.0	26
495	Tunable Crystallinity and Charge Transfer in Twoâ€Dimensional Gâ€Quadruplex Organic Frameworks. Angewandte Chemie - International Edition, 2018, 57, 3985-3989.	7.2	26
496	The nonadiabaticity question for europium(III/II): outer-sphere reactivities of europium(III/II) cryptates. Inorganic Chemistry, 1983, 22, 3465-3470.	1.9	25
497	Environmentally induced multiple intervalence transitions in a symmetrically substituted analog of the Creutz-Taube ion. Inorganic Chemistry, 1992, 31, 157-160.	1.9	25
498	Luminescent Ruthenium Polypyridyl Complexes Containing Pendant Pyridinium Acceptors. Inorganic Chemistry, 1996, 35, 3719-3722.	1.9	25
499	How Far Do Electrons Move? A Semiempirical Investigation of Thermal Electron-Transfer Distances in Cationic Bis(hydrazine) and Bis(hydrazyl) Mixed-Valence Compounds. Journal of the American Chemical Society, 2001, 123, 2053-2057.	6.6	25
500	Shape-selective transport through rectangle-based molecular materials: Thin-film scanning electrochemical microscopy studies. Proceedings of the National Academy of Sciences of the United States of America, 2002, 99, 5171-5177.	3.3	25
501	Isomer of linker for NU-1000 yields a new she -type, catalytic, and hierarchically porous, Zr-based metal–organic framework. Chemical Communications, 2021, 57, 3571-3574.	2.2	25
502	Electrochromic devices based on thin metallopolymeric films. Solar Energy Materials and Solar Cells, 1992, 25, 315-325.	3.0	24
503	Synthesis and Characterization of Hexametallic Molecular Hosts Featuring Large Cavity Volumes and Constrained Cavity Port Sizes. Molecular Crystals and Liquid Crystals, 2000, 342, 151-158.	0.3	24
504	Monitoring Molecular Adsorption on High-Area Titanium Dioxide via Modulated Diffraction of Visible Light. Langmuir, 2001, 17, 3109-3112.	1.6	24

#	Article	IF	CITATIONS
505	Metal–Organic Frameworks Containing (Alkynyl)Gold Functionalities: A Comparative Evaluation of Solvent-Assisted Linker Exchange, <i>de Novo</i> Synthesis, and Post-synthesis Modification. Crystal Growth and Design, 2014, 14, 6320-6324.	1.4	24
506	Enhanced Gas Sorption Properties and Unique Behavior toward Liquid Water in a Pillared-Paddlewheel Metal–Organic Framework Transmetalated with Ni(II). Inorganic Chemistry, 2014, 53, 10432-10436.	1.9	24
507	Atomic Layer Deposition of Rhenium–Aluminum Oxide Thin Films and ReO _{<i>x</i>} Incorporation in a Metal–Organic Framework. ACS Applied Materials & Interfaces, 2017, 9, 35067-35074.	4.0	24
508	Vibrational Coherence Due to Promoting Mode Activity in the Relaxation Dynamics of the Class III Mixed-Valence Molecule [Ru2TIEDCl4]+. Journal of Physical Chemistry A, 2002, 106, 1131-1143.	1.1	23
509	Theoretical insights into direct methane to methanol conversion over supported dicopper oxo nanoclusters. Catalysis Today, 2018, 312, 2-9.	2.2	23
510	Electroactive Ferrocene at or near the Surface of Metal–Organic Framework UiO-66. Langmuir, 2018, 34, 4707-4714.	1.6	23
511	Supramolecular Porous Organic Nanocomposites for Heterogeneous Photocatalysis of a Sulfur Mustard Simulant. Advanced Materials, 2020, 32, e2001592.	11.1	23
512	An iron-porphyrin grafted metal–organic framework as a heterogeneous catalyst for the photochemical reduction of CO2. Journal of Photochemistry and Photobiology, 2022, 10, 100111.	1.1	23
513	Direct Observation of Modulated Radical Spin States in Metal–Organic Frameworks by Controlled Flexibility. Journal of the American Chemical Society, 2022, 144, 2685-2693.	6.6	23
514	Surface environmental effects in electrochemical kinetics: Outer-sphere chromium(III) reductions at mercury, gallium, lead, and thallium surfaces. Journal of Electroanalytical Chemistry and Interfacial Electrochemistry, 1984, 179, 219-238.	0.3	22
515	Crown ether functionalization of a porphyrin-based "molecular squareâ€i induction of fluorescence sensitivity to alkali metal cations. Synthetic Metals, 2001, 117, 215-217.	2.1	22
516	Luminescent infinite coordination polymer materials from metal-terpyridine ligation. Dalton Transactions, 2011, 40, 9189.	1.6	22
517	Evaluation of a robust, diimide-based, porous organic polymer (POP) as a high-capacity sorbent for representative chemical threats. Journal of Porous Materials, 2012, 19, 261-266.	1.3	22
518	Tuning the Hydrophobicity of Zinc Dipyridyl Paddlewheel Metal–Organic Frameworks for Selective Sorption. Crystal Growth and Design, 2013, 13, 2938-2942.	1.4	22
519	Enhancement of the Yield of Photoinduced Charge Separation in Zinc Porphyrin–Quantum Dot Complexes by a Bis(dithiocarbamate) Linkage. Journal of Physical Chemistry C, 2015, 119, 5195-5202.	1.5	22
520	Utility of Surface Reaction Entropies for Examining Reactantâ€Solvent Interactions at Electrochemical Interfaces. Ferriciniumâ€Ferrocene Attached to Platinum Electrodes. Journal of the Electrochemical Society, 1984, 131, 619-622.	1.3	21
521	Electron-transfer reactions in mixed solvents. An electrochemical probe of unsymmetrical selective solvation. Inorganic Chemistry, 1989, 28, 3786-3790.	1.9	21
522	lonic Association Effects upon Optical Electron Transfer Energetics: Studies in Water with (CN)5Fell-BPE-FellI(CN)55 Inorganic Chemistry, 1994, 33, 4446-4452.	1.9	21

#	Article	IF	CITATIONS
523	Anodic aluminium oxide catalytic membranes for asymmetric epoxidation. Chemical Communications, 2005, , 5331.	2.2	21
524	Effect of secondary substituent on the physical properties, crystal structures, and nanoparticle morphologies of (porphyrin)Sn(OH)2: diversity enabled via synthetic manipulations. Journal of Materials Chemistry, 2008, 18, 3640.	6.7	21
525	Computational Study of Propylene and Propane Binding in Metal–Organic Frameworks Containing Highly Exposed Cu ⁺ or Ag ⁺ Cations. Journal of Physical Chemistry C, 2014, 118, 9086-9092.	1.5	21
526	Liquidâ€Phase Epitaxially Grown Metal–Organic Framework Thin Films for Efficient Tandem Catalysis Through Siteâ€Isolation of Catalytic Centers. ChemPlusChem, 2016, 81, 708-713.	1.3	21
527	SALEâ€Ing a MOFâ€Based "Ship of Theseus.―Sequential Buildingâ€Block Replacement for Complete Reformulation of a Pillaredâ€Paddlewheel Metalâ€Organic Framework. European Journal of Inorganic Chemistry, 2016, 2016, 4345-4348.	1.0	21
528	Assembly of dicobalt and cobalt–aluminum oxide clusters on metal–organic framework and nanocast silica supports. Faraday Discussions, 2017, 201, 287-302.	1.6	21
529	Application and Limitations of Nanocasting in Metal–Organic Frameworks. Inorganic Chemistry, 2018, 57, 2782-2790.	1.9	21
530	Stabilizing a Vanadium Oxide Catalyst by Supporting on a Metal–Organic Framework. ChemCatChem, 2018, 10, 1772-1777.	1.8	21
531	Atomic layer deposition of Pt@CsH2PO4 for the cathodes of solid acid fuel cells. Electrochimica Acta, 2018, 288, 12-19.	2.6	21
532	The Molecular Path Approaching the Active Site in Catalytic Metal–Organic Frameworks. Journal of the American Chemical Society, 2021, 143, 20090-20094.	6.6	21
533	Entropic driving-force effects upon preexponential factors for intramolecular electron transfer: implications for the assessment of nonadiabaticity. Inorganic Chemistry, 1984, 23, 256-258.	1.9	20
534	Photoeffects in thin-film molecular-level chromophore-quencher assemblies. 1. Physical characterization. The Journal of Physical Chemistry, 1989, 93, 294-304.	2.9	20
535	X-ray Nanoscale Profiling of Layer-by-Layer Assembled Metal/Organophosphonate Films. Langmuir, 2004, 20, 8022-8029.	1.6	20
536	Photoinduced electron transfer from rail to rung within a self-assembled oligomeric porphyrin ladder. Chemical Communications, 2010, 46, 547-549.	2.2	20
537	Electron transfer rates from time-dependent correlation functions. Wavepacket dynamics, solvent effects, and applications. Journal of Photochemistry and Photobiology A: Chemistry, 1994, 82, 87-101.	2.0	19
538	High Resolution Assembly of Patterned Metal Oxide Thin Films via Microtransfer Molding and Electrochemical Deposition Techniques. Electrochemical and Solid-State Letters, 1999, 2, 175.	2.2	19
539	Transient DC Photocurrent Investigation of Charge Redistribution within Re(CO)3Cl(2,2â€ [~] -bipyridine): An Unexpected Decrease in Molecular Dipole Moment upon Emissive Excited-State Formation. Inorganic Chemistry, 2000, 39, 1817-1819.	1.9	19
540	An Inorganic Application of Transient Direct Current Photoconductivity: Corroboration of a Charge-Transfer Assignment for the Luminescing States of Pt(dpphen)(ecda)1. Inorganic Chemistry, 2000, 39, 1814-1816.	1.9	19

#	Article	IF	CITATIONS
541	Comparative X-ray Standing Wave Analysis of Metalâ^'Phosphonate Multilayer Films of Dodecane and Porphyrin Molecular Square. Journal of Physical Chemistry B, 2005, 109, 1441-1450.	1.2	19
542	Solvent-induced configuration mixing and triplet excited-state inversion: insights from transient absorption and transient dc photoconductivity measurements. Physical Chemistry Chemical Physics, 2009, 11, 8586.	1.3	19
543	A zwitterionic metal–organic framework with free carboxylic acid sites that exhibits enhanced hydrogen adsorption energies. CrystEngComm, 2013, 15, 9408.	1.3	19
544	Porphyrins as Templates for Site-Selective Atomic Layer Deposition: Vapor Metalation and in Situ Monitoring of Island Growth. ACS Applied Materials & Interfaces, 2016, 8, 19853-19859.	4.0	19
545	Encapsulating CdSe/CdS QDs in the MOF ZIF-8 Enhances Their Photoluminescence Quantum Yields in the Solid State. Chemistry of Materials, 2022, 34, 1921-1929.	3.2	19
546	Incorporation of free halide ions stabilizes metal–organic frameworks (MOFs) against pore collapse and renders large-pore Zr-MOFs functional for water harvesting. Journal of Materials Chemistry A, 2022, 10, 6442-6447.	5.2	19
547	Photocurrents arising from photolysis of synthetically controlled chromophore—quencher structures in polymeric films. Journal of Electroanalytical Chemistry and Interfacial Electrochemistry, 1985, 190, 287-291.	0.3	18
548	Electroabsorption and Related Spectroscopic Studies of Bimetallic Tetraiminoethylenedimacrocyclic Complexes:  Corroboration of Valence Electron Delocalization. Inorganic Chemistry, 1998, 37, 2837-2840.	1.9	18
549	Two coordinatively linked supramolecular assemblies constructed from highly electron deficient porphyrins. Inorganica Chimica Acta, 2004, 357, 4005-4014.	1.2	18
550	Isobutane Dehydrogenation over Bulk and Supported Molybdenum Sulfide Catalysts. Industrial & Engineering Chemistry Research, 2020, 59, 1113-1122.	1.8	18
551	Investigating the Process and Mechanism of Molecular Transport within a Representative Solvent-Filled Metal–Organic Framework. Langmuir, 2020, 36, 10853-10859.	1.6	18
552	Two-Dimensional Pd Rafts Confined in Copper Nanosheets for Selective Semihydrogenation of Acetylene. Nano Letters, 2021, 21, 5620-5626.	4.5	18
553	Temperature effects for localized versus delocalized optical intervalence transitions. Journal of the American Chemical Society, 1993, 115, 6428-6429.	6.6	17
554	Nature of the Interaction and Photophysical Properties of [Mo6Cli8(SO3CF3)a6]2- and [Mo6Cli8Cla6]2- on Silica Gel. Chemistry of Materials, 1995, 7, 43-49.	3.2	17
555	High-Surface-Area Architectures for Improved Charge Transfer Kinetics at the Dark Electrode in Dye-Sensitized Solar Cells. ACS Applied Materials & Interfaces, 2014, 6, 8646-8650.	4.0	17
556	Vapor-Phase Cyclohexene Epoxidation by Single-Ion Fe(III) Sites in Metal–Organic Frameworks. Inorganic Chemistry, 2021, 60, 2457-2463.	1.9	17
557	Tuning the Conductivity of Hexa-Zirconium(IV) Metal–Organic Frameworks by Encapsulating Heterofullerenes. Chemistry of Materials, 2021, 33, 1182-1189.	3.2	17
558	Regioselective Functionalization of the Mesoporous Metal–Organic Framework, NU-1000, with Photo-Active Tris-(2,2′-bipyridine)ruthenium(II). ACS Omega, 2020, 5, 30299-30305.	1.6	17

#	Article	IF	CITATIONS
559	Understanding Diffusional Charge Transport within a Pyrene-Based Hydrogen-Bonded Organic Framework. Langmuir, 2022, 38, 1533-1539.	1.6	17
560	Sensing via optical interference. Materials Today, 2005, 8, 46-52.	8.3	16
561	Powered by porphyrin packing. Nature Materials, 2015, 14, 1192-1193.	13.3	16
562	Calcium Vapor Adsorption on the Metal–Organic Framework NU-1000: Structure and Energetics. Journal of Physical Chemistry C, 2016, 120, 16850-16862.	1.5	16
563	Ni(ii) complex on a bispyridine-based porous organic polymer as a heterogeneous catalyst for ethylene oligomerization. Catalysis Science and Technology, 2017, 7, 4351-4354.	2.1	16
564	Nickel–Carbon–Zirconium Material Derived from Nickel-Oxide Clusters Installed in a Metal–Organic Framework Scaffold by Atomic Layer Deposition. Langmuir, 2018, 34, 14143-14150.	1.6	16
565	Molybdenum Sulfide within a Metal–Organic Framework for Photocatalytic Hydrogen Evolution from Water. Journal of the Electrochemical Society, 2019, 166, H3154-H3158.	1.3	16
566	Structural reversibility of Cu doped NU-1000 MOFs under hydrogenation conditions. Journal of Chemical Physics, 2020, 152, 084703.	1.2	16
567	Reduction of 1,3-dimethyl-5-(p-nitrophenylimino)barbituric acid by thiols. A high-velocity flavin model reaction with an isolable intermediate. Journal of the American Chemical Society, 1979, 101, 1890-1893.	6.6	15
568	The influence of lead underpotential deposition on the capacitance of the silver-aqueous interface. Journal of Electroanalytical Chemistry and Interfacial Electrochemistry, 1982, 131, 299-307.	0.3	15
569	Solvent-dependent redox thermodynamics as a probe of solvent shielding in lanthanide cryptates. Inorganic Chemistry, 1986, 25, 1916-1918.	1.9	15
570	Dynamics of Back Electron Transfer in Dye-Sensitized Solar Cells Featuring 4- <i>tert</i> -Butyl-Pyridine and Atomic-Layer-Deposited Alumina as Surface Modifiers. Journal of Physical Chemistry B, 2015, 119, 7162-7169.	1.2	15
571	Toward a Charged Homo[2]catenane Employing Diazaperopyrenium Homophilic Recognition. Journal of the American Chemical Society, 2018, 140, 6540-6544.	6.6	15
572	Photoeffects in thin-film molecular-level chromophore-quencher assemblies. 2. Photoelectrochemistry. The Journal of Physical Chemistry, 1989, 93, 304-313.	2.9	14
573	Modulation of photoinduced electron-transfer reactivity by intramolecular folding. Journal of the American Chemical Society, 1993, 115, 2048-2049.	6.6	14
574	Extended Near-Infrared Resonance Raman Investigations of an Organic Mixed-Valence System:Â Diazatetracyclodiene Radical Cation. Journal of Physical Chemistry A, 1999, 103, 11172-11180.	1.1	14
575	Microvisualization of Structural Features and Ion Electroinsertion Behavior of Patterned WO[sub 3] Thin Films via Integrated Optical and Atomic Force Microscopies. Electrochemical and Solid-State Letters, 1999, 2, 497.	2.2	14
576	Luminescence-based assessment of thermodynamic constants for electrostatic binding of non-luminescent dyes and atomic ions to colloidal semiconductor surfaces. Journal of Photochemistry and Photobiology A: Chemistry, 2001, 143, 251-256.	2.0	14

#	Article	IF	CITATIONS
577	Excess Polarizability Reveals Exciton Localization/Delocalization Controlled by Linking Positions on Porphyrin Rings in Butadiyne-Bridged Porphyrin Dimers. Journal of Physical Chemistry A, 2010, 114, 3384-3390.	1.1	14
578	Determining the Conduction Band-Edge Potential of Solar-Cell-Relevant Nb ₂ O ₅ Fabricated by Atomic Layer Deposition. Langmuir, 2017, 33, 9298-9306.	1.6	14
579	Catalytically Active Silicon Oxide Nanoclusters Stabilized in a Metal–Organic Framework. Chemistry - A European Journal, 2017, 23, 8532-8536.	1.7	14
580	Electron-transfer reactions in water. Contributions from high-frequency librations?. The Journal of Physical Chemistry, 1987, 91, 1001-1003.	2.9	13
581	What optical electron-transfer reactions can teach us about electrode kinetics and electrocatalysis. Langmuir, 1989, 5, 696-706.	1.6	13
582	Electrochemical, spectral, and quartz crystal microgravimetric assessment of conduction band edge energies for nanocrystalline zirconium dioxide/solution interfaces. Coordination Chemistry Reviews, 2004, 248, 1225-1230.	9.5	13
583	Combining solvent-assisted linker exchange and transmetallation strategies to obtain a new non-catenated nickel (II) pillared-paddlewheel MOF. Inorganic Chemistry Communication, 2016, 67, 60-63.	1.8	13
584	Characterization of metal-complex-containing organic polymeric films by secondary ion mass spectrometry. Analytical Chemistry, 1986, 58, 2443-2447.	3.2	12
585	Solvents Effects on the Efficacy of Recognition of Amminemetal Complexes by Macrocyclic Ethers: In situ Probes of Extent of Encapsulation. Inorganic Chemistry, 1994, 33, 4738-4743.	1.9	12
586	Electron Self-Exchange Kinetics for a Water-Soluble Ferrocenium/Ferrocene Couple:Â Rate Modulation via Charge Dependent Calix[6]arene-p-sulfonate Encapsulation. Inorganic Chemistry, 1996, 35, 1402-1404.	1.9	12
587	Epoxidation of the Commercially Relevant Divinylbenzene with [<i>tetrakis</i> -(Pentafluorophenyl)porphyrinato]iron(III) Chloride and Its Derivatives. Industrial & Engineering Chemistry Research, 2015, 54, 922-927.	1.8	12
588	Singleâ€Site, Singleâ€Metalâ€Atom, Heterogeneous Electrocatalyst: Metal–Organicâ€Framework Supported Molybdenum Sulfide for Redox Mediatorâ€Assisted Hydrogen Evolution Reaction. ChemElectroChem, 2020, 7, 509-516.	1.7	12
589	Art of Architecture: Efficient Transport through Solvent-Filled Metal–Organic Frameworks Regulated by Topology. Chemistry of Materials, 2021, 33, 6832-6840.	3.2	12
590	Redox thermodynamics of surface-bound reactants. Journal of Electroanalytical Chemistry and Interfacial Electrochemistry, 1984, 163, 371-379.	0.3	11
591	Selective recognition of metal complexes by macrocyclic ethers: further observations on the macrocycle size dependence and the first-sphere ligand composition dependence of recognition thermodynamics. Inorganica Chimica Acta, 1995, 240, 285-289.	1.2	11
592	Synthesis and Characterization of the New Selenometalate Anion [Ir(Se4)3]3 Inorganic Chemistry, 1995, 34, 5101-5102.	1.9	11
593	On the mechanism of oxidative electropolymerization and film formation for phenanthroline-containing complexes of ruthenium. Journal of Electroanalytical Chemistry, 1996, 414, 23-29.	1.9	11
594	Synthesis and photophysical properties of luminescent rhenium(I) and manganese(I) polypyridine complexes containing pendant 1,3,4-oxadiazole/triarylamine assemblies. Inorganica Chimica Acta, 2001, 318, 53-60.	1.2	11

#	Article	IF	CITATIONS
595	Molecular Sieving and Thin Film Transport by Molecular Materials Featuring Large Component Cavities. Electrochemical and Solid-State Letters, 2002, 5, E25.	2.2	11
596	Electron Transfer in Platinum(II) Diimine-Centered Triads: Mechanistic Insights from Photoinduced Transient Displacement Current Measurements. Journal of Physical Chemistry A, 2009, 113, 6430-6436.	1.1	11
597	The Role of Electronic Coupling in Linear Porphyrin Arrays Probed by Singleâ€Molecule Fluorescence Spectroscopy. Chemistry - A European Journal, 2011, 17, 9219-9225.	1.7	11
598	Cyclic metalloporphyrin dimers and tetramers: tunable shape-selective hosts for fullerenes. Dalton Transactions, 2012, 41, 12156.	1.6	11
599	Squeezing the box: isoreticular contraction of pyrene-based linker in a Zr-based metal–organic framework for Xe/Kr separation. Dalton Transactions, 2020, 49, 6553-6556.	1.6	11
600	Double-Walled Zn ₃₆ @Zn ₁₀₄ Multicomponent Senary Metal–Organic Polyhedral Framework and Its Isoreticular Evolution. Journal of the American Chemical Society, 2021, 143, 17942-17946.	6.6	11
601	Selective-solvation-induced intramolecular electron transfer: time resolution via pulsed accelerated flow spectrophotometry. Journal of the American Chemical Society, 1992, 114, 7957-7958.	6.6	10
602	fac-Tricarbonylchlorobis(pyridine-N)rhenium andfac-Tricarbonylchlorobis(4,4'-bipyridine-N)rhenium. Acta Crystallographica Section C: Crystal Structure Communications, 1998, 54, 1596-1600.	0.4	10
603	Manipulation of the distance of light-induced electron transfer within a semi-rigid donor(amine)/acceptor(terpyridine) assembly via complexation of di-positive and tri-positive metal ions. Journal of Electroanalytical Chemistry, 2003, 554-555, 449-458.	1.9	10
604	Tunable Crystallinity and Charge Transfer in Twoâ€Đimensional Gâ€Quadruplex Organic Frameworks. Angewandte Chemie, 2018, 130, 4049-4053.	1.6	10
605	Extending the Compositional Range of Nanocasting in the Oxozirconium Cluster-Based Metal–Organic Framework NU-1000—A Comparative Structural Analysis. Chemistry of Materials, 2018, 30, 1301-1315.	3.2	10
606	Engineering Dendrimer-Templated, Metal–Organic Framework-Confined Zero-Valent, Transition-Metal Catalysts. ACS Applied Materials & Interfaces, 2021, 13, 36232-36239.	4.0	10
607	Toward molecular selectivity with chemically modified electrodes: can electroactivity and permeability through an overlaying metallopolymer film be controlled via rational manipulation of internal architecture?. Journal of Electroanalytical Chemistry, 1995, 397, 119-126.	1.9	9
608	Nonadiabatic electron transfer at the nanoscale tin-oxide semiconductor/aqueous solution interfaceDedicated to Professor Fred Lewis on the occasion of his 60th birthday Photochemical and Photobiological Sciences, 2004, 3, 240.	1.6	9
609	Manganese porphyrin multilayer films assembled on ITO electrodes via zirconium phosphonate chemistry: chemical and electrochemical catalytic oxidation activity. Topics in Catalysis, 2005, 34, 101-107.	1.3	9
610	Barrier-Layer-Mediated Electron Transfer from Semiconductor Electrodes to Molecules in Solution: Sensitivity of Mechanism to Barrier-Layer Thickness. Journal of Physical Chemistry C, 2016, 120, 20922-20928.	1.5	9
611	Transport Diffusion of Linear Alkanes (C ₅ –C ₁₆) through Thin Films of ZIF-8 as Assessed by Quartz Crystal Microgravimetry. Langmuir, 2021, 37, 9405-9414.	1.6	9
612	Liquid/Liquid Interface Polymerized Porphyrin Membranes Displaying Size-Selective Molecular and Ionic Permeability. Langmuir, 2006, 22, 1804-1809.	1.6	8

#	Article	IF	CITATIONS
613	Probing Exciton Localization/Delocalization: Transient dc Photoconductivity Studies of Excited States of Symmetrical Porphyrin Monomers, Oligomers, and Supramolecular Assemblies. Journal of Physical Chemistry A, 2009, 113, 8182-8186.	1.1	8
614	Catalysis at the Organic Ligands. RSC Catalysis Series, 2013, , 289-309.	0.1	8
615	Single-Atom Metal Oxide Sites as Traps for Charge Separation in the Zirconium-Based Metal–Organic Framework NDC–NU-1000. Energy & Fuels, 0, , .	2.5	8
616	Identifying the Polymorphs of Zr-Based Metal–Organic Frameworks via Time-Resolved Fluorescence Imaging. , 2022, 4, 370-377.		8
617	Multielectron-transfer kinetics for cis- versus trans-dioxorhenium(V) species: isoelectronic modeling with osmium(VI/V) and control of interfacial reactivity by rhenium(IV) accessibility. Inorganic Chemistry, 1992, 31, 3879-3881.	1.9	7
618	Resonance Raman spectroscopic studies of trans-dioxorhenium(V) tetrapyridyl species. Inorganic Chemistry, 1992, 31, 5143-5145.	1.9	7
619	Ion modulated electroactivity in thin-film polymers derived from bipyridyl and phenanthroline complexes of iron. Journal of Electroanalytical Chemistry, 1995, 387, 109-113.	1.9	7
620	Vapor permeation studies of membranes made from molecular squares. Journal of Membrane Science, 2003, 221, 103-111.	4.1	7
621	Research Update: A hafnium-based metal-organic framework as a catalyst for regioselective ring-opening of epoxides with a mild hydride source. APL Materials, 2014, 2, .	2.2	7
622	Does the Mode of Metal–Organic Framework/Electrode Adhesion Determine Rates for Redox-Hopping-Based Charge Transport within Thin-Film Metal–Organic Frameworks?. Journal of Physical Chemistry C, 2022, 126, 4601-4611.	1.5	7
623	Some Comparisons Between the Energetics of Electrochemical and Homogeneous Electron-Transfer Reactions. ACS Symposium Series, 1982, , 181-212.	0.5	6
624	A polymer-film based photoelectrode containing immobilized quencher and chromophore polymer blends. Journal of Electroanalytical Chemistry and Interfacial Electrochemistry, 1987, 224, 59-65.	0.3	6
625	Electrochemical assembly of multicomponent, redox-conductive metallopolymeric films with arbitrary three-dimensional control over macroscopic structure and chemical composition. Journal of Electroanalytical Chemistry and Interfacial Electrochemistry, 1989, 261, 423-429.	0.3	6
626	Solvational Barriers to Interfacial Electron Transfer: Minimization via Valence Delocalization. The Journal of Physical Chemistry, 1995, 99, 853-855.	2.9	6
627	Ethylene polymerization with a crystallographically well-defined metal–organic framework supported catalyst. Catalysis Science and Technology, 2022, 12, 1619-1627.	2.1	6
628	BODIPY-Based Polymers of Intrinsic Microporosity for the Photocatalytic Detoxification of a Chemical Threat. ACS Applied Materials & amp; Interfaces, 2022, 14, 12596-12605.	4.0	6
629	Carbon-efficient conversion of natural gas and natural-gas condensates to chemical products and intermediate feedstocks <i>via</i> catalytic metal–organic framework (MOF) chemistry. Energy and Environmental Science, 2022, 15, 2819-2842.	15.6	6
630	Unexpected oxidative electropolymerization of ruthenium phenanthroline complexes of 4,4'-bipyridine and bis(pyridyl)ethylene. Journal of Electroanalytical Chemistry and Interfacial Electrochemistry, 1988, 251, 417-420.	0.3	5

#	Article	IF	CITATIONS
631	Photoredox pathways to spatially restricted metallopolymeric films. Inorganic Chemistry, 1992, 31, 1540-1542.	1.9	5
632	Spectroscopic and photophysical studies of apparent cluster-to-organic-acceptor charge transfer in a molecular cadmium sulfide assembly. Chemical Physics Letters, 1996, 251, 84-89.	1.2	5
633	Investigating the effect of metal nuclearity on activity for ethylene hydrogenation by metal-organic-framework-supported oxy-Ni(II) catalysts. Journal of Catalysis, 2022, 407, 162-173.	3.1	5
634	Photoeffects in thin film chromophore-quencher assemblies: variations in the light absorber. Journal of Photochemistry and Photobiology A: Chemistry, 1989, 48, 419-433.	2.0	4
635	Unexpected redox rectification by an electrochemically prepared iridium oxide electrode/aqueous acid interface. Journal of Electroanalytical Chemistry, 1993, 345, 351-362.	1.9	4
636	Mode-specific quantum rate effects for interfacial electron transfer: computational case studies based upon 4-cyano-N-methylpyridinium reduction. Journal of the Chemical Society, Faraday Transactions, 1996, 92, 3909.	1.7	4
637	A Crown-Linked Donor–Acceptor Assembly Containing ReI(diimine)(CO)3Cl and Nitrobenzene Components. Acta Crystallographica Section C: Crystal Structure Communications, 1997, 53, 1054-1055.	0.4	4
638	Phosphonates Meet Metalâ^'Organic Frameworks: Towards CO 2 Adsorption. Israel Journal of Chemistry, 2018, 58, 1164-1170.	1.0	4
639	Structural effects in electron transfer reactions: comparative interfacial electrochemical kinetics for cis- versus trans-dioxorhenium(V)(bi)pyridine oxidation. Journal of Electroanalytical Chemistry, 1995, 380, 229-235.	1.9	3
640	Resonance Raman and Semiempirical Electronic Structure Studies of an Odd-Electron Dinickel Tetraiminoethylenedimacrocycle Complex. Inorganic Chemistry, 2000, 39, 3911-3914.	1.9	3
641	Contrasting electroabsorbance behavior of two borderline class II/class III mixed-valence systems. Chemical Physics, 2005, 319, 28-38.	0.9	3
642	Synthesis and Characterization of Functionalized Metal-organic Frameworks. Journal of Visualized Experiments, 2014, , e52094.	0.2	3
643	Engendering Long-Term Air and Light Stability of a TiO ₂ -Supported Porphyrinic Dye via Atomic Layer Deposition. ACS Applied Materials & Interfaces, 2016, 8, 34863-34869.	4.0	3
644	Correction to "Tuning Zr ₆ Metal-Organic Framework (MOF) Nodes as Catalyst Supports: Site Densities and Electron-Donor Properties Influence Molecular Iridium Complexes as Ethylene Conversion Catalysts― ACS Catalysis, 2018, 8, 2364-2364.	5.5	3
645	Sinterâ€Resistant Platinum Catalyst Supported by Metal–Organic Framework. Angewandte Chemie, 2018, 130, 921-925.	1.6	3
646	An Adduct Between Tetraammine(1,10-phenanthroline)ruthenium(II) and Dibenzo-42-crown-14. Acta Crystallographica Section C: Crystal Structure Communications, 1998, 54, 1427-1431.	0.4	2
647	Electrochemistry in Nanostructered Inorganic Molecular Materials. Materials Research Society Symposia Proceedings, 2001, 676, 151.	0.1	2
648	Transparent Conducting Oxides at High Aspect Ratios by ALD. ECS Transactions, 2006, 3, 243-247.	0.3	2

#	Article	IF	CITATIONS
649	Correction to "Computationally Guided Discovery of Catalytic Cobalt-Decorated Metal–Organic Framework for Ethylene Dimerization― Journal of Physical Chemistry C, 2017, 121, 11975-11975.	1.5	2
650	Solvent and Temperature Effects in Mixed-Valence Chemistry. , 1991, , 51-66.		2
651	Photo-Induced Electron Transfer Reactivity at NanoscaleSemiconductor-Solution Interfaces. , 2003, , .		2
652	Stabilization of Low Valent Zirconium Nitrides in Titanium Nitride via Plasma-Enhanced Atomic Layer Deposition and Assessment of Electrochemical Properties. ACS Applied Energy Materials, 2020, 3, 5095-5100.	2.5	2
653	Redox-Hopping-Based Charge Transport Mediated by Ru(II)-Polypyridyl Species Immobilized in a Mesoporous Metal-Organic Framework. Frontiers in Chemical Engineering, 2022, 3, .	1.3	2
654	A method for evaluating the surface concentrations of two like-charged ions simultaneously adsorbed at an electrode-solution interface. Journal of Electroanalytical Chemistry and Interfacial Electrochemistry, 1984, 167, 275-279.	0.3	1
655	Interfacial Polymerization of Molecular Squares: Thin Microporous Membranes Featuring Size Selective Transport. Materials Research Society Symposia Proceedings, 2002, 734, 111.	0.1	1
656	Molecular Squares, Boxes, and Cubes. , 2004, , 909-916.		1
657	Adding to the Arsenal of Zirconium-Based Metal-Organic Frameworks:theTopology as a Platform for Solvent-Assisted Metal Incorporation. European Journal of Inorganic Chemistry, 2016, 2016, 4266-4266.	1.0	1
658	Correction to "Surface Modification of SnO2 Photoelectrodes in Dye-Sensitized Solar Cells: Significant Improvements in Photovoltage via Al2O3 Atomic Layer Deposition― Journal of Physical Chemistry Letters, 2011, 2, 824-824.	2.1	0
659	The Balance between Conductivity and Electro-/Photo-Catalytic Performance of Guest-Incorporated Metal-Organic Frameworks. ECS Meeting Abstracts, 2021, MA2021-01, 786-786.	0.0	0
660	(Invited) Toward MOF-Enabled Solar Cells. Light Harvesting, Energy Transport, Exciton Splitting, and Delivery of Electrons to Electrodes or Catalysts. ECS Meeting Abstracts, 2021, MA2021-01, 1765-1765.	0.0	0
661	Effect of the organic cation on 2D organic-inorganic Perovskites. , 0, , .		0
662	Charge transfer in mixed and segregated stacks of tetrathiafulvalene, tetrathianaphthalene and naphthalene diimide: a structural, spectroscopic and computational study. New Journal of Chemistry, 0, , .	1.4	0